



UNIVERSIDADE FEDERAL DO RIO GRANDE-FURG
INSTITUTO DE CIÊNCIAS BIOLÓGICAS (ICB)
DISSERTAÇÃO DE MESTRADO
PROGRAMA DE PÓS-GRADUAÇÃO EM
CIÊNCIAS FISIOLÓGICAS

**Efeitos do grafeno através de diferentes rotas de exposição
considerando dois modelos biológicos (*Litopenaeus vannamei* e *Danio
rerio*).**

Bióloga Amanda Lucena Fernandes

Dissertação apresentada para o Programa de Pós-Graduação em Ciências Fisiológicas, como parte dos requisitos para obtenção do título de MESTRE em Ciências Fisiológicas sob a Orientação da Profa. Dra. Juliane Ventura Lima e Co-orientação do Prof. Dr. José Maria Monserrat.

RIO GRANDE

2017.

Agradecimentos

Gostaria de iniciar agradecendo a todos aqueles que me ajudaram a executar esse trabalho ao longo desses mais de dois anos, seja no laboratório, nas aulas teóricas ou nos momentos de crise existencial que acho que todo pós-graduando passa por pelo menos uma vez na vida. Aos meus amigos fora do mundo científico que incentivaram e sempre estiveram ao meu lado para ajudar ou descontraír, não citarei nomes, mas tenho certeza que os especiais sabem quem são.

Não posso deixar de agradecer ao meu namorado Pedro, a quem amo e está ao meu lado nesses quase 10 anos, me aturando nos momentos de chatice, de reclamação, de alegria, de estresse e que sempre não mede esforços para me ajudar e apoiar, obrigada.

Aos meus “babys” animais que amo, minha felina Angie que está comigo desde a prova para entrar no mestrado, passando noites estudando para provas, escrevendo projetos e claro deitando em cima das folhas; e ao “catoros” Kael e Bruce, que se revelaram verdadeiros grudes nesse período de escrita, atrapalhando um pouco às vezes, mas que são como de terapia de vida.

A minha família, que sempre me apoiou em minhas decisões e me incentivou a sempre buscar o melhor para mim, avós e avôs, pai e mãe, obrigada a vocês.

Por último gostaria de agradecer a minha orientadora Juliane, como ela diz a melhor orientadora de todas. Já são quatro anos juntas, desde a graduação, muito aprendi contigo Jú, conhecimentos tantos profissionais como pessoais que vou levar para a vida. Obrigada por tudo, saiba que te admiro muito como pessoa como profissional também, pelo modo de trabalhar assim como pelo relacionamento com seus orientados.

Sumário

| | |
|--|----|
| 1. Resumo | 4 |
| 2. Abstract | 6 |
| 3. Introdução | 8 |
| 3.1 Características físico-químicas do grafeno..... | 8 |
| 3.2 Diferentes rotas de exposição e efeitos do grafeno | 10 |
| 3.3 Modelos biológicos..... | 12 |
| 4. Objetivos | 15 |
| 4.1 Objetivos gerais | 15 |
| 4.2 Objetivos específicos..... | 15 |
| 5. Capítulo 1 (Artigo 1) | 17 |
| 6. Capítulo 2 (Manuscrito 2) | 52 |
| 7. Discussão geral | 87 |
| 8. Bibliografia geral | 90 |

1. Resumo

. O grafeno (GR) é um NM de carbono que tem ganhado grande destaque devido à suas características físico-químicas, que o permitem ser utilizado nas indústrias tecnológicas, farmacológicas e biomédicas. Ele possui formato de folha e é formado por uma camada bidimensional de carbono (2D), sua utilização se deve a grande estabilidade térmica, elétrica e química. Com o aumento do uso deste NM, é fundamental analisar se o provável descarte em ambientes aquáticos pode induzir efeitos tóxicos nos organismos vivos. Uma vez no ambiente, os animais podem ser expostos através de diferentes rotas de exposição como o ar, água e alimentação e exercer efeitos tóxicos nestes organismos. Diante destes fatos, o objetivo do presente estudo foi investigar os efeitos tóxicos do grafeno através de diferentes rotas de exposição (injeção intraperitoneal e alimentação) em animais aquáticos de diferentes ambientes (água doce e marinho) e se sua exposição é capaz de induzir estresse oxidativo nestes animais.

A presente dissertação é composta por dois estudos distintos, no primeiro estudo, camarões *Litopenaeus vannamei* foram expostos durante quatro semanas à concentração de grafeno de 500 mg/kg de ração e foram avaliados efeitos em brânquias, hepatopâncreas e músculo. Os resultados bioquímicos mostraram alteração do sistema de defesa antioxidante, com um aumento da concentração de glutathiona reduzida (GSH) e da capacidade antioxidante total contra radicais peroxil, além de um aumento da concentração das espécies reativas de oxigênio (ROS), em brânquias e hepatopâncreas; aumento da atividade da enzima glutamato cisteína ligase (GCL) no hepatopâncreas e diminuição nas brânquias; enquanto que o hepatopâncreas mostrou um decréscimo na atividade da glutathiona-S-transferase (GST) e um acréscimo em brânquias. Nos dois tecidos citados acima também foram encontrados danos oxidativo lipídicos, e alterações

26 de DNA sendo observada a capacidade de genotoxicidade do grafeno. Também, os
27 resultados histopatológicos mostraram mudanças na morfologia do hepatopâncreas após
28 a exposição ao grafeno, como hiperplasia das células basais, infiltração de hemócitos e
29 decréscimo de células secretoras.

30 O segundo estudo avaliou as respostas toxicológicas da exposição intraperitoneal
31 de 5 e 50 mg/L de grafeno no peixe *Danio rerio* durante 48 h em brânquias, intestino,
32 músculo e cérebro. Os resultados analisando biomarcadores moleculares de estresse
33 oxidativo, mostrou que os genes *nrf2* e *gclc* (subunidade catalítica da enzima GCL) não
34 sofreram alteração em sua expressão após a exposição, enquanto que o sistema
35 antioxidante enzimático do animal foi alterado em alguns tecidos após a exposição.
36 Após a exposição de 5mg de GR/L, a concentração de GSH em brânquias diminuiu,
37 enquanto que mostrou um aumento no intestino e em cérebro, sendo este resultado
38 também observado após exposição a 50 mg/L no cérebro. A atividade da enzima GCL
39 foi induzida após a exposição a ambos os grupos de GR em intestino e cérebro, já na
40 enzima GST foi observado um acréscimo de atividade após a exposição de 5 mg/L de
41 GR nestes mesmos tecidos. Danos a macromoléculas como lipídios foram observados
42 em brânquias após a exposição à maior concentração; como também alterações
43 morfológicas em brânquias, cérebro e músculo com histopatologias de grau moderado a
44 severo, apresentando hiperplasia, inflamações e edemas nos tecidos.

45 Com estes estudos evidencia-se a capacidade do grafeno em produzir efeitos
46 tóxicos para estes animais aquáticos, seja em uma exposição direta (*i.p*) ou através da
47 alimentação por curta ou longa exposição. Como não existe hoje uma legislação que
48 controle a liberação de nanomateriais de carbono no ambiente, e com o crescente uso
49 dos mesmos, estudos sobre esses efeitos se torna importante para contribuir níveis de
50 segurança para os seres vivos presentes nestes ambientes.

51 2. Abstract

52 Graphene (GR) is a carbon NM that has been having higher prominence due to
53 their physical-chemical characteristics, which are used in the technological,
54 pharmacological and biomedical industries. It has a sheet shape and consists of a one
55 layer of carbon (2D), possessing high thermal, electrical and chemical stability. With
56 increased use of this NM, it becomes necessary to analyze if their disposal in aquatic
57 environments are not causing toxic effects for living organisms. Once into environment,
58 the animals can be exposed through different routes of exposition such as air, water and
59 food and cause toxic effects in these organisms. Considering these facts, the objective of
60 this study was to investigate the toxic effects of graphene through different exposure
61 routes (intraperitoneal injection and food) in aquatic animals from different
62 environments (freshwater and marine) and their possibility of induce oxidative stress in
63 these animals.

64 This dissertation is composed by two different studies, in the first study, the
65 animals were exposed for four weeks to graphene concentration of 500 mg/kg of ration
66 and changes in gills, hepatopancreas and muscle of *Litopenaeus vannamei* were
67 evaluated. Biochemical results showed changes of the antioxidant defense system, with
68 an increase in the concentration of reduced glutathione (GSH) and the total antioxidant
69 capacity against peroxy radicals, besides an increase of reactive oxygen species (ROS)
70 concentration in gills and hepatopancreas; increase glutamate cysteine ligase (GCL)
71 activity in hepatopancreas and decrease in gills; while hepatopancreas showed a
72 decrease in glutathione-S-transferase (GST) activity and an increase in gills. In the
73 tissues mentioned above were also observed lipid oxidative damages, and alterations in
74 DNA, being observed genotoxicity of graphene. Histopathological results showed

75 changes in the morphology of hepatopancreas after exposure to graphene, such as basal
76 cell hyperplasia, hemocyte infiltration and decrease of secretory cell.

77 The second study evaluated the toxicological responses of intraperitoneal
78 exposure at 5 and 50mg GR/L in *Danio rerio* for 48 h in gills, intestine, muscle and
79 brain. The results of molecular biomarkers of oxidative stress showed that *nrf2* and *gclc*
80 genes (catalytic subunit of the GCL enzyme) did not change their expression after
81 exposure, while the enzymatic antioxidant system of the animal was altered in some
82 tissues. After exposure to 5 mg GR/L, the concentration of GSH in gills decreased,
83 while in intestine and brain increased, the same result also was observed in brain after
84 exposure to 50 mg GR/L. The activity of the GCL enzyme was induced after exposure
85 to both GR groups in the intestine and brain, whereas an increase in the GST activity
86 was observed after exposure of 5 mg GR/L in these same tissues. Damage to
87 macromolecules such as lipids were observed in gills after exposure at the highest
88 concentration, also were observed morphological changes in gills, brain and muscle
89 with moderate to severe histopathology, presenting hyperplasia, inflammations and
90 edema in tissues.

91 It those studies the ability of graphene to produce toxic effects for aquatic
92 animals were demonstrated, either being by a direct (i.p) or through feed exposure
93 during a short or long exposure time. Currently, there is no legislation that controls the
94 release of carbon nanomaterials into the environment, and these materials are
95 increasingly being used, the study of these effects becomes important to contribute with
96 levels of safety for present living beings in this environment.

97 3. Introdução

98 3.1 Características físico-químicas do grafeno

99 Os nanomateriais (NM) são partículas com tamanho que varia de 1 a 100 nm em
100 pelo menos uma dimensão. Estes NM estão sendo amplamente utilizados para novas
101 tecnologias em diversas áreas como as biológicas, farmacológicas, da saúde e na
102 informática (Aitken et al., 2006; Oberdörster, 2004). Eles podem ser incorporados,
103 metabolizados pelos organismos através da água, dieta e/ou por inalação, se distribuindo
104 em diferentes órgãos, entrando em contato com tecidos e células e podendo assim, se
105 acumular e causar efeitos tóxicos nos mesmos (Fischer & Chan, 2007; Park et al., 2011;
106 Zhang et al., 2011). Deste modo, os NM podem interagir com moléculas como o DNA
107 além de induzir a produção de espécies reativas de oxigênio (ROS) que possuem a
108 capacidade de reagir com estrutura de proteínas e lipídios de membrana, induzir danos
109 ao DNA e modular respostas antioxidantes (Lee et al., 2008; Matés et al., 1999). Esta
110 geração de ROS pode ser atribuída a fatores como concentração, tempo de exposição,
111 tipo de dispersante utilizado junto ao NM, além do tipo de funcionalização dos mesmos
112 (Aitken et al., 2006). Além disso, os NM tendem a se agregar em soluções aquosas
113 devido à carga eletrostática do NM, além da força iônica presente no meio. Em
114 contrapartida, muitas vezes a funcionalização aumenta sua biocompatibilidade e
115 solubilidade podendo deste modo, reduzir sua citotoxicidade e genotoxicidade, assim
116 polímeros e moléculas são utilizados para a modificação destes NM (Firme & Bandaru
117 2010; Liu et al, 2011 (a); Pan et al, 2012)

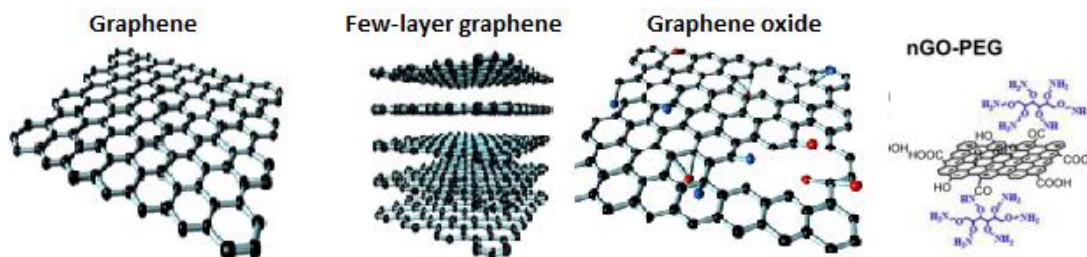
118 O grafeno (GR) é um nanomaterial formado por uma única camada de átomos de
119 carbono possuindo duas dimensões com uma estrutura planar semelhante a uma folha
120 (*nanosheets*) (Mafra, 2008). Por possuir propriedades físico-químicas de grande
121 interesse para o campo tecnológico, como sua grande área de superfície, alta

122 condutividade elétrica e estabilidade térmica, óptica, química e eletroquímica; seu uso
123 tem crescido nos últimos anos (Chen et. al, 2010; Huang e Shi, 2012). A produção de
124 GR pode ser realizada por vários métodos, entretanto a forma mais utilizada é através da
125 exfoliação do grafite, devido a seu custo baixo e a facilidade de produção (Latin e
126 Henrard, 2006). Na estrutura do GR, cada átomo de carbono está ligado a outro átomo
127 de carbono (carbono-carbono) no mesmo plano, fazendo desta uma forte ligação, o que
128 lhe dá a característica de um dos materiais mais resistente descoberto até o presente
129 momento (Syama e Mohanan, 2016).

130 O GR hoje compõe uma família de NM (**Figura 1**), que foram funcionalizados e
131 modificados para atender diferentes demandas. A natureza do GR é hidrofóbica,
132 portanto, quando entra em contato com soluções aquosas a tendência é que o material
133 sofra agregação; para superar esse problema o óxido de grafeno (GO) foi desenvolvido,
134 através da adição de grupos químicos reativos como epóxi (–O–), hidroxila (–OH) e
135 ácido carboxílico (–COOH), gerando pontas hidrofílicas no NMs, aumentando desta
136 forma a superfície além de possuir poucas folhas de grafite permitindo certa
137 maleabilidade ao material, pois a resistência acaba sendo diminuída (Kiew et al., 2016;
138 Park et al., 2009; Texter, 2014). Contudo, a presença destes grupos proporciona uma
139 redução em suas propriedades químicas, térmicas e física, o que faz do GR um melhor
140 material para se utilizar no âmbito tecnológico (Karlický. 2013).

141 Outra forma de funcionalização do GR é a adição de estruturas que modifiquem a
142 superfície deste NM, incluindo polímeros hidrofílicos como o polietileno glicol (PEG)
143 que é o mais utilizado; esta funcionalização melhora a dispersão e estabilidade do NM
144 em soluções aquosas (Kiew et al., 2016). Estudos biológicos e farmacológicos têm
145 utilizado este tipo de NM funcionalizado principalmente como carreador de fármacos,

146 devido a melhor circulação destes no sangue, além de melhor biodistribuição em
147 diferentes órgãos do animal, quando comparado com a forma pristina do GR (Yang et
148 al., 2013). Por outro lado, também devido à diferença em estruturas e grupamentos
149 químicos presente nestes NM, ocorre uma alteração na capacidade de penetração e
150 ligação destes NM nos diferentes compartimentos celulares, podendo exercer efeitos
151 tóxicos (Jortner e Rao, 2002; Liu et al., 2011 (b)).



152

153 **Figura 1.** Diferentes formas químicas de grafeno (Adaptado de Kiew et al. (2016) e Yang et al.
154 (2013)).

155

156 3.2 Diferentes rotas de exposição e efeitos do grafeno

157 O ambiente aquático engloba uma grande fauna, onde vertebrados e invertebrados
158 estão constantemente expostos a qualquer tóxico nele presente, sendo suscetível à
159 contaminação, pois a maioria dos contaminantes têm como destino final as grandes
160 massas de água (Mieiro et al., 2011). Uma das formas de avaliar os efeitos de
161 contaminantes ambientais nos organismos vivos é analisar parâmetros bioquímicos de
162 estresse oxidativo, toda vez que uma grande variedade de compostos tóxicos possa
163 direta ou indiretamente alterar defesas antioxidantes e exacerbar o dano oxidativo
164 (Monserrat et al., 2007; Ventura-Lima et al., 2009). Além de parâmetros bioquímicos
165 enzimáticos, a expressão de genes que codificam para enzimas e moléculas
166 antioxidantes relacionadas ao estresse oxidativo é outro método muito utilizado para

167 analisar os efeitos gerados por exposição a diferentes tóxicos, considerando-se que os
168 organismos podem estar respondendo a um nível molecular que pode anteceder algumas
169 respostas bioquímicas, apesar do oposto ocorrer mais comumente (Storey, 2005; White
170 et al., 2003).

171 Com a crescente utilização do GR pode também surgir risco de exposição dos
172 organismos, principalmente aquáticos, através das mais variadas rotas de exposição, as
173 frequentemente escolhidas para estudos toxicológicos, englobam exposições em água,
174 via alimentação (**Figura 2**) e injeções intraperitoneais (*i.p.*) do material diretamente no
175 animal (**Figura 3**) (Zhang et al., 2016). O tipo escolhido de exposição pode influenciar
176 em muito nos resultados de um estudo, sendo que as exposições via água e sedimento
177 geralmente estão associadas a recriar situações ambientais reais de contaminação.
178 Efeitos tóxicos do óxido de grafeno quando exposto na água *Danio rerio* foram
179 avaliados por Chen et al. (2016), onde os autores observaram alterações em enzimas do
180 sistema oxidante como superóxido dismutase (SOD) e catalase (CAT), além de alterar
181 os níveis de glutathiona reduzida (GSH) e induzir a expressão de genes de citocinas
182 inflamatórias, caracterizando uma situação geral de estresse oxidativo.



183
184

Figura 2: Exposição via ração de grafeno

Figura 3: Exposição intraperitoneal de grafeno

185 Assim como a rota de exposição aquática, as exposições orais tentam recriar
186 situações que poderiam ocorrer no meio ambiente. Porém, poucos são os estudos com
187 GR que utilizaram esta rota de exposição, por exemplo, Mao et al. (2016) observaram

188 que após exposição oral em ratos, o GR causou edema nos pulmões, porém estes efeitos
189 foram transitórios, e nenhum grande dano foi observado. Exposições *i.p.* de GR foram
190 realizadas em alguns estudos (Dziewiecka et al., 2016; Kurantowicz et al., 2015;
191 Strojny et al., 2015; Yang et al., 2013), e foram observados efeitos tóxicos na maioria
192 dos experimentos, com alterações morfológicas em tecidos e modificação na atividade
193 de enzimas ou moléculas do animal. Esse tipo de exposição geralmente é escolhido
194 quando se quer testar uma dose exata do contaminante, pois, sabe-se que NM podem ser
195 comportar diferentemente quando em contato com soluções aquosas (da Rocha et al.,
196 2013).

197 Estudos sobre o comportamento do grafeno em contato com células, mostram que
198 este NM age em nível de membrana, sendo de difícil penetração nas células,
199 provavelmente alterando as propriedades de membrana devido a morfologia plana em
200 2D, levando a uma alteração na solubilidade e gerando produção de espécies reativas de
201 oxigênio (Lee et al., 2008; Nguyen e Berry, 2012). A toxicidade do óxido de grafeno em
202 células foi exemplificada em estudo, onde a morte de bactérias foi causada pelo
203 aumento de ROS dentro das células bacterianas (Liu et al., 2011 (c)).

204 **3.3 Modelos biológicos**

205 A escolha do modelo biológico em um experimento é de extrema importância,
206 principalmente para experimentos toxicológicos, onde vários fatores precisam ser
207 considerados: a espécie não pode ser frágil, precisa ser de fácil manutenção e pequena
208 para haver um transporte facilitado, se tratando de espécies aquáticas que precisam ser
209 realocadas de aquários; além de precisar se adequar a análise de diferentes tipos de
210 estressores químicos (He et al., 2014).

211 O crustáceo *Litopenaeus vannamei*, conhecido como camarão branco do Pacífico,
212 é uma espécie costeira de clima tropical, com ocorrência na costa do Pacífico, América
213 Central e Sul, das Antilhas ao Rio Grande do Sul- RG. Possui ciclo de vida migratório,
214 onde os adultos são encontrados em regiões marinhas de até 30 metros de profundidade
215 e os juvenis em estuários, baías e enseadas (Iawi, 1973; Perez-Farfante, 1969; Silva,
216 1977). A espécie é de grande importância econômica, sendo amplamente cultivada para
217 o comércio em diferentes regiões do globo, como América, China e Tailândia, assim
218 utilizada para o consumo humano, devido a isso, a espécie tem sido escolhida cada vez
219 mais para estudos toxicológicos, visto que pode ser uma fonte de contaminação para o
220 consumidor final (Yang et al., 2010).

221 Além disso, a espécie possui características que a tornam um bom modelo para
222 estudos toxicológicos, como grandes taxas de sobrevivência e adaptação a diferentes
223 condições físico-químicas, como diferenças de salinidade e temperatura (Lotz, 2003).
224 Por isso *L. vannamei* tem se mostrando um bom modelo biológico para estudos que
225 avaliam os efeitos de diferentes contaminantes ambientais (Ren et al., 2015 (a,b);
226 Lobato et al., 2013), entre eles contaminantes emergentes, como os NM (Juarez-Moreno
227 et al., 2017).

228 O peixe *Danio rerio*, conhecido como zebrafish, é uma espécie comumente
229 utilizada em experimentos de pesquisa científica devido a seu baixo custo e rápido
230 desenvolvimento, genoma muito semelhante ao de mamíferos, assim como órgãos e
231 tecidos, considerando aspectos anatômicos, fisiológicos, moleculares e celulares (He et
232 al., 2014; Lawrence, 2007). A espécie também é um bom modelo para estudo de
233 toxicidade, sendo usada em estudos com contaminantes ambientais e NM, pois mostra
234 respostas de toxicidade para um amplo espectro de materiais como, por exemplo, NM
235 de carbono; exibem respostas fisiológicas a xenobióticos semelhantes ao que ocorre em

236 mamíferos, como produção de enzimas antioxidantes para combater o estresse
237 oxidativo; e devido ao genoma ser semelhante ao de mamíferos, possuem respostas
238 fisiológicas e imunológicas equivalentes (Fako e Furgeson, 2009; Froehlicher et al.,
239 2009; Pyati et al., 2007).

240 Devido a isso, a espécie se tornou a principal alternativa para testes de saúde
241 humana e avaliação de riscos ecológicos por contaminantes potenciais (Esch et al.,
242 2012). De fato, estudos demonstraram a toxicidade de nanomateriais de carbono em *D.*
243 *rerio*, quando expostos a nanotubos de carbono e fulereno C₆₀, induzindo um cenário de
244 estresse oxidativo, com alterações do sistema antioxidante (da Rocha et. al, 2013;
245 Usenko et al., 2008). Além disso, devido ao seu tamanho pequeno, avaliações
246 histopatológicas de todos os órgãos do animal podem ser feitas facilmente e com baixo
247 custo, o que é uma vantagem em relações a outras espécies de peixes utilizadas em
248 experimentos toxicológicos, como *Cyprinus carpio* (Esch et al., 2012).

249 Entretanto, estudos analisando a toxicidade do GR tanto em zebrafish, como em
250 outros seres vivos, atualmente é limitado, com poucos dados presentes na literatura,
251 onde os já publicados analisam outras formas de grafeno, como por exemplo, o óxido de
252 grafeno (Yang et al., 2013). Desta forma torna-se necessário o conhecimento da
253 toxicidade apresentada por este NM considerando-se o constante aumento do uso do
254 mesmo nos últimos anos.

255

256 4. Objetivos

257 4.1 Objetivo geral

258 Avaliar os efeitos toxicológicos do grafeno considerando diferentes rotas de
259 exposição em organismos aquáticos de ambientes marinho e dulciaquícola.

260

261 4.2 Objetivos específicos

262 Associado a exposição do grafeno incorporado à ração no crustáceo *Litopenaeus*
263 *vannamei* (Crustacea, decápoda):

264 • Avaliar a concentração de ROS e níveis de peroxidação lipídica nas brânquias,
265 hepatopâncreas e músculo dos animais.

266 • Analisar os efeitos em parâmetros bioquímicos associados às defesas
267 antioxidantes como: níveis de glutathione reduzida (GSH), atividade das enzimas
268 relacionadas com a GSH (glutathione-S-transferase, glutamato cisteína ligase) e
269 capacidade antioxidante total no músculo, hepatopâncreas e brânquias.

270 • Avaliar a indução de genotoxicidade em brânquias, hepatopâncreas e músculo.

271 • Analisar os efeitos histopatológicos em brânquias, hepatopâncreas e músculo.

272 Associado a exposição intraperitoneal de grafeno em *Danio rerio* (Cyprinidae)

273 • Analisar a expressão de genes associados à resposta antioxidante como o fator *nrf2*
274 (fator nuclear eritróide 2) e *gclc* (subunidade catalítica da enzima GCL) em
275 brânquias, intestino, e músculo de *D. rerio*.

276 • Avaliar se a exposição altera parâmetros de atividade antioxidante e estresse
277 oxidativo incluindo níveis de glutathione reduzida (GSH), atividade das enzimas:
278 glutamato cisteína ligase (GCL) e glutathione-S-transferase (GST) e dano oxidativo
279 lipídico em brânquias, intestino, músculo e cérebro.

- 280 • Analisar os efeitos histopatológicos do grafeno em brânquias, intestino, músculo
281 e cérebro.

5. Capítulo 1

Exposure to few-layers graphene through diet induces oxidative stress and histological changes in the marine shrimp *Litopenaeus vannamei*.

Manuscript accepted in *Toxicology Research*

(Fator de impacto: 2.161)

Amanda Lucena Fernandes^{1,2}, Marcelo Estrella Josende^{1,2}, Jefferson Patrício Nascimento⁴, Adelina Pinheiro Santos⁴, Sangram Keshai Sahoo⁴, Flávio Manoel Rodrigues da Silva Júnior^{1,3}, Luis Alberto Romano⁵, Clascídia Aparecida Furtado⁴, Wilson Wasielesky⁵, José Maria Monserrat^{1,2,5},
Juliane Ventura-Lima^{1,2*}.

¹Instituto de Ciências Biológicas (ICB), Universidade Federal do Rio Grande - FURG, Rio Grande, RS, Brasil.

²Programa de Pós-Graduação em Ciências Fisiológicas - FURG.

³Programa de Pós-Graduação em Ciências da Saúde- FURG

⁴Centro de Desenvolvimento da Tecnologia Nuclear – CDTN/CNEN, Belo Horizonte, MG, Brazil.

⁵Programa de Pós-Graduação em Aquicultura-FURG.

* Corresponding author: Juliane Ventura-Lima

Phone/Fax: +55 5332935249

E-mail: juliane_ventura@pesquisador.cnpq.br

Abstract

282 The production and use of graphene-based nanomaterials is rapidly increasing.
283 However, little data are available regarding the toxicity of these nanomaterials in
284 aquatic organisms. In the present study, the toxicity of few-layer graphene (FLG)
285 (obtained by chemical exfoliation) was evaluated in different tissues of the shrimp
286 *Litopenaeus vannamei* following exposure through diet for four weeks. Transmission
287 electron microscopy and dynamic light scattering measurements showed a distribution
288 of lateral sheet sizes between 100 and 2000 nm with average length and width of 800
289 and 400 nm, respectively. Oxidative stress parameters were analyzed, indicating that
290 FLG exposure led to an increase in the concentration of reactive oxygen species,
291 modulated the activity of antioxidant enzymes such as glutamate cysteine ligase and
292 glutathione-S-transferase, and reduced glutathione levels and total antioxidant capacity.
293 However, observed modulations were not sufficient to avoid lipid and DNA damage in
294 both gill and hepatopancreas tissues. Further, graphene exposure resulted in
295 morphological changes in hepatopancreas tissues. These results demonstrate that
296 exposure to FLG through diet induces alterations in the redox state of cells, leading to a
297 subsequent oxidative stress situation. It is therefore clear that this nanomaterial
298 presenting these physico-chemical characteristics may be harmful to aquatic biota.

299 **Key-words:** few-layer graphene, nanotoxicology, oxidative stress, shrimp,
300 antioxidant responses.

301

1. Introduction

Nanotechnology is expanding rapidly, and various nanomaterials (NM) are already being applied in technological and biomedical areas (Powell et al., 2010). Considering the growing production and use of these NM, their release into aquatic environments and interaction with biological systems appears inevitable (Handy et al., 2011). It is important to understand the effects NM may have on aquatic organisms, and to infer the potential ecotoxicological risks for ecosystems (Matranga and Corsi, 2012).

Graphene is an allotrope of carbon composed of a single two-dimensional layer (2D), which possesses unique electrical, mechanical, thermal and optical properties (Zhang et al., 2011). Different production processes have been proposed to explore each of these properties, using different experimental routes and yielding graphene-based materials with different physicochemical characteristics. Characteristics such as the number of graphene layers, average lateral size, and carbon-to-oxygen (C/O) atomic ratio may be modified. Graphene-based materials comprise not only single-layer graphenes but also few-layer graphenes (i.e., 2–10 layers), graphene oxide, reduced graphene oxide, graphite nanoplatelets (i.e., more than 10 graphene sheets but below 100 nm in thickness), graphene ribbons, graphene dots and other derivatives. The physicochemical characteristics of a graphene-based material can determine its integration into biological media and the environment, and consequently its toxicity to organisms and ecosystems. For example, graphene oxide and reduced graphene oxide were found to be readily accumulated by cells and exert toxicity on biological models. Specifically, these materials induced the generation of reactive oxygen species (ROS), modulation of antioxidant system and oxidative damage in lipids and DNA (Chatterjee et al., 2014). Further, acute exposure (24 h) to two different graphenes in the crustacean *Artemia salina* induced oxidative stress, evidenced by alterations in the antioxidant

327 system and lipid peroxidation. This toxicity increased as nanoparticle sizes decreased
328 (Pretti et. al., 2014).

329 Carbon nanomaterials (CNM) tend to deposit in sediment, as predicted by
330 environmental modeling by Gottschalk et al. (2009). This deposition likely endangers
331 organisms that live in close proximity to sediment. In fact, Waisse-Leinonen and co-
332 authors (2012) showed that fullerene (C₆₀) exerts toxicity on the benthic organism
333 *Chironomus riparius* after contact with contaminated sediment. Diet represents another
334 environmentally relevant exposure route, as NM tends to adsorb to surfaces such as in
335 food matter, and are subsequently ingested by organisms (Zhu et. al., 2010).

336 The Pacific white shrimp *Litopenaeus vannamei* (Crustacea, Decapoda) is a
337 species widely distributed along the Pacific Coast and in South and Central America
338 and possess high economic value as they are a main species employed in shrimp
339 farming around the world (Wang et al., 2015). Beyond this, *L. vannamei* exhibit a high
340 tolerance to stressful conditions and has been used extensively in toxicological studies
341 (Lobato et al., 2013).

342 Until now, few studies have assessed the toxicity of graphene-based materials on
343 aquatic organisms. The objective of the present study was to evaluate the toxicological
344 effects of exposure to chemically exfoliated FLG via diet in *L. vannamei*. Specifically,
345 oxidative stress parameters and histological alterations in different tissues of shrimps
346 were analyzed. The authors present that this is the first study evaluating the toxicity of
347 this NM through dietary exposure in a benthic species such as *L. vannamei*.

348

2. Materials and Methods

2.1. Obtainment and characterization of FLG

FLG was obtained according to the work of Khan and co-authors (2011). This procedure was performed with the following two major steps. In the first step, 3.3 g of natural graphite (Graflake 99580, supplied by Nacional de Grafite LTDA-Brazil) was added to 1000 mL of NMP (1-methyl-2-pyrrolidinone, Sigma-Aldrich). This mixture was then placed in an ultrasonic bath (Cole-Parmer 08895-50 –100 – 250 W a 42 kHz) and sonicated for 168 h. The mixture was then centrifuged (Heraeus Multifuge X1R) at 110 g for 45 min. The supernatant was collected (around 90% of flask volume) and filtered through a nylon membrane (0.2 μm diameter). A washing was performed using 400 mL deionized water, 200 mL of ethanol (95% P.A) and 100 mL of diethyl ether (Synth P.A) in order to remove waste NMP. FLG was dried for 24 h at 150°C under vacuum. In the second step, the dried FLG obtained in the first step was added to 16 mL of NMP (1-methyl-2-pirrolyde; 24 mg.mL⁻¹) and sonicated for 24 h. Posteriorly, the dispersion obtained was kept standing for 8 days and the supernatant was collected and filtered through a 0.2 μm membrane. Again, the material was washed as described above. Finally, the derived sample of FLG was dried for 24 h at 150 °C under vacuum.

The morphology, structure and size of exfoliated FLG were characterized by transmission electron microscopy (TEM), Raman spectroscopy and dynamic light scattering (DLS). Images of TEM were collected in a microscope (Tecnai G2–Spirit- FEI-2006) operated with tension of 80 kV. A drop of supernatant was collected in step 2 (described above) and deposited over a copper grid covered with carbon film (holey carbon 300 mesh) and dried for 24 h under vacuum at room temperature. Raman spectroscopy was performed in Raman Horiba Jobin Yvon iHR 550 using a 514 nm laser (2.41 eV), 4.6 mW power, three accumulations of 60 s and objective of 50 x. For

374 Raman measurements, a drop of supernatant collected in step 2 was deposited and
375 diluted 100 x in NMP over substrate of Si/SiO₂, dried under vacuum for 24 h at 150 °C.
376 DLS measurements were carried out using a Zetasizer Nano ZS equipped with a laser of
377 633 nm.

378 **2.2. Diet supplemented with graphene nanosheets.**

379 The FLG concentration used was 500 mg/kg of ration; the nanomaterial in power
380 was mixed to the feed previously macerated and this mixture subsequently was sealed
381 with 3.3% bovine gelatin (Sigma-Aldrich, Inc.) and MilliQ water the bovine gelatin was
382 used to avoid that the FLG was released from ration. Following this procedure, the feed
383 (FLG or control) was dried in an oven at 50 °C and then stored in glass vials at 4°C. A
384 control diet was prepared in the same way but was not supplemented with graphene.
385 The choice of FLG nanosheet concentration was based on work analyzing the effect of
386 carbon nanomaterials in the diet of *Oncorhynchus mykiss* by Fraser et al. (2011).

387 **2.3. Detection of graphene in the ration**

388 To identify if the incorporation of FLG in the feed had been efficient, was
389 performed vibrational spectral measurements of control and FLG supplemented food
390 samples were carried out using Raman spectroscopy in the near IR (NIR) region of the
391 electromagnetic spectrum to detected FLG into the ration. The Raman experiments were
392 carried out using a Bruker RFS 100/S Fourier Transform (FT) Raman spectrometer in
393 macro sampling mode with a 1064 nm excitation source from a Nd:YAG laser attached
394 to a liquid nitrogen cooled Ge detector. The choice of NIR excitation wavelength helps
395 in maintaining low noise as well as an effective rejection of naturally occurring
396 unwanted food autofluorescence. Laser power and spectrometer resolution were kept at
397 150 mW and 4 cm⁻¹, respectively, for the spectral acquisition for 256 scans. Control and

398 FLG subjected food samples were ground to a fine powder using a mortar and pestle,
399 sandwiched between two glass cover slips and exposed to the laser focus in the sample
400 chamber. The resultant spectrum was chosen on the basis of average of the spectra
401 acquired for each sample.

402 **2.4. Maintenance of *L. vannamei* shrimps**

403 A total of 64 animals (~ 15 g each) were obtained from Marine Station of
404 Aquaculture (EMA) of the Federal University of Rio Grande (FURG) and immediately
405 transferred to laboratory. Animals were then acclimated in a tank of 100 L of seawater
406 for at least two weeks prior to the beginning of the experiment. The shrimps were fed
407 twice day with commercial ration (45% crude protein) under laboratory conditions
408 (temperature of 20 °C and photoperiod of 12 hours light/12 hours dark with a screen
409 shading for stress reduction in the animals, pH 8.0, and constant aeration in order to
410 maintain dissolved oxygen at 7.2 mg O₂/L). No mortality was observed during the
411 acclimation period.

412 **2.5. Experimental design**

413 Two replicates were performed in this study, and in each replicate, the animals
414 were divided into two experimental groups: **1) Treatment group (n=8 per aquarium in
415 duplicate):** received ration supplemented with FLG (as described previously), and **2)
416 Control group (n=8 per aquarium in duplicate):** received ration without FLG. All
417 experimental groups were fed twice per day. Each group was maintained in aquarium
418 with 10 L of seawater with constant aeration (7.2 mg O₂/L) and pH 8.0. The quantity of
419 feed offered to animals was based on 2.8% of the average weight of animals per
420 aquarium. Shrimps were weighed weekly during all experiment periods for adjustments

421 in the quantity of ration offered over four weeks (exposure period). There was no
422 mortality in both groups during exposure time.

423 **2.6. Biochemical analysis**

424 **2.6.1. Preparation of homogenates**

425 After each experiment the animals were sacrificed via freezing, while gill,
426 hepatopancreas and muscle tissues were immediately removed and stored at -80°C.
427 Tissues were homogenized (1:4 w/v) in crustacean homogenization buffer (Tris-base
428 buffer (20 mM) with sucrose (0.5 M), EDTA (20 mM), DDT (1 mM), KCl (0.15 mM))
429 and protease inhibitor cocktail (Sigma-Aldrich), with pH adjusted to pH 7.75. After
430 homogenization, samples were centrifuged at 10,000 x g at 4 °C for 20 min.
431 Supernatants were then aliquoted and stored (-80 °C) for assays of enzyme activities,
432 concentration of reduced glutathione (GSH), total antioxidant capacity and lipid
433 peroxidation. However ROS determination was performed with fresh tissue
434 immediately after dissection.

435 Measurements of enzymatic activities were standardized by the total amount of
436 protein present in the extracts. Measurements of total protein concentration were
437 performed using the commercial kit based on the Biuret method with microplate reader
438 (ELX 800 Biotel) at 550 nm.

439 **2.6.2. Determining the concentration of reactive oxygen species (ROS)**

440 For ROS detection, 2',7' dichlorofluorescein diacetate (H₂DCF-DA) probe was
441 used, which generates a detectable fluorochrome at wavelengths of 485 and 530 nm for
442 excitation and emission, respectively (Viarengo et al., 1999) (after deacetylation and in

443 the presence of ROS). The readings were performed with microplate reader (Victor 2
444 fluorometer, Perkin Elmer).

445 **2.6.3. Enzymatic assays and reduced glutathione (GSH) levels**

446 The methodology for glutamate cysteine ligase (GCL) activity and GSH levels
447 was based on White et al. (2003). This analysis is based on the ability of the compound
448 2,3-naphthalenedicarboxaldehyde (NDA) to react with γ -glutamylcysteine (γ -GC) or
449 glutathione (GSH), forming a fluorescent cyclic compound (GC-NDA and GS-NDA,
450 respectively). The fluorescence of the complex NDA- γ -GC and GS-NDA was
451 measured using a fluorometer (2 Victor, Perkin Elmer) with wavelengths of 485 and
452 530 nm for excitation and emission respectively.

453 Glutathione-S-transferase (GST) activity was determined according to Habig et al.
454 (1974). This analysis measures the conjugation of 1 mM GSH (Sigma) with 1 mM of
455 the reagent 1-chloro-2,4-dinitrobenzene (CDNB, Sigma), a reaction catalyzed by GST.
456 The complex formed has a maximum absorbance at 340 nm. Absorbance was measured
457 using a microplate reader (Victor2, Perkin Elmer).

458 **2.6.4. Determination of lipid peroxidation and total antioxidant capacity**

459 Lipid peroxidation was measured fluorometrically via the thiobarbituric acid
460 reactive substance (TBARS) method in accordance with Oakes and Kraak (2003). This
461 method involves the reaction of malondialdehyde (MDA), a degradation by-product of
462 peroxidized lipids, with thiobarbituric acid (TBA) under conditions of high temperature
463 and acidity, resulting in a detectable fluorescent chromogen (wavelength of 520 nm
464 (excitation) and 580 nm (emission)). Tetramethoxypropane (TMP, Sigma) was used as
465 a standard and MDA content was expressed as nmol of TMP equivalent/mg of protein.

466 The total antioxidant capacity against peroxy radicals was assessed following the
467 protocol of Amado et al. (2009). This analysis consists of the thermal decomposition of
468 ABAP (2,2'-azobis (2-methylpropionamide dihydrochloride) at 37 °C, which
469 generates peroxy radicals. 2', 7' dichlorofluorescein diacetate (H₂DCF-DA) was added
470 before reading, as this compound reacts with esterases to produce a non-fluorescent
471 compound (H₂DCF). This is subsequently oxidized by ROS, generating a fluorescent
472 compound that is detectable at a wavelength of 485 and 530 for excitation and emission
473 respectively. The calculation of total antioxidant capacity is based on a second order
474 polynomial function that integrates ROS area with or without ABAP. In this way,
475 smaller area corresponds with greater antioxidant capacity due to
476 neutralization/interception of peroxy radicals.

477 **2.6.5. DNA damage**

478 DNA damage was assessed by an alkaline version of the comet assay, according
479 to Singh et al. (1998). Aliquots (15 uL) of muscle, hepatopancreas and gill tissue
480 homogenates were mixed with low melting point agarose (37 °C) and placed on slides
481 containing agarose. These were left in lysis buffer for at least 2 h, after which
482 electrophoresis was conducted under the following conditions: 30V (1 V / cm), 300 mA,
483 20 min in an ice bath. Slides were stained with SYBR Safe and analyzed using a
484 fluorescence microscope. The % DNA in tail, the tail length and tail moment of
485 nucleoids (100 per animal) were analyzed using ImageJ software.

486 **2.7. Histological analysis**

487 Whole animal bodies were fixed by injection of Davidson solution. Different parts
488 of the shrimps were kept immersed in the same solution for 24 h. Afterward, body
489 sections corresponding with muscle, gill and hepatopancreas tissues were cut away and

490 were processed in an automatic tissue processor LUPE PT 05 (dehydration, rinsing,
491 clearing and impregnation) and embedded in Paraplast (Sigma-Aldrich). Following
492 embedment, the tissues were sectioned in microtome (LUPETEC MRPO3) with 4 μm
493 thin sections. The sections were stained with hematoxylin and eosin (H&E). A light
494 optic microscope (Primo star, Zeiss) was used to analyze the histological cuts, and the
495 images were captured using a 400x magnification camera (ERc5s, AxioCam). 5 animals
496 were used in both experimental groups (control and FLG), and two histological sections
497 were measured for each shrimp. The analyses were performed by a single-board
498 certified medical pathologist.

499 **3. Statistical analysis**

500 Statistical differences were tested using one-way analysis of variance (ANOVA)
501 followed by Tukey *post hoc* comparison. Normality and variance were previously
502 checked and mathematical transformations were made where necessary. The
503 significance level was fixed at 5% for all statistical analyses (Zar, 1984).

504 **4. Results**

505 TEM images confirmed exfoliated graphene sheets as mostly with rectangular
506 shape and well-defined borders (**Figure 1a, b and c**). The nanosheets were
507 agglomerated in several regions due to the deposition process and drying of samples
508 over the TEM grid (Figure 1a). **Figure 1d** shows the statistics of the lateral dimensions
509 of 150 nanosheets measured from several TEM images. A large distribution of sheet
510 sizes between 100 nm and 2000 nm with average length and width values of 800 and
511 400 nm, respectively, can be observed in the histogram. The distribution of the
512 hydrodynamic diameter found by DSL ranged from 200 to 1000 nm (data adjusted

513 according to Lotya (2013), with average diameter of 500 nm (**Figure 1e**). These
514 represent results of the same order of distribution magnitude found via TEM.

515 The efficiency of the exfoliation of the natural graphite to graphenes, as well as
516 the structural quality of the nanosheets obtained, was evaluated by Raman spectroscopy
517 with excitation in the visible range (**Figure 1f**). Raman spectra display the characteristic
518 bands of graphenic structures: G band ($\sim 1580\text{ cm}^{-1}$) assigned to primarily in-plane C=C
519 vibrational mode, D band ($\sim 1350\text{ cm}^{-1}$) activated by disorder and G' ($\sim 2700\text{ cm}^{-1}$)
520 assigned to the second order overtone of D band. The increase of the I_D/I_G ratio (0.39)
521 for the exfoliated graphene compared with the I_D/I_G ratio (0.09) for the natural graphite
522 (0.09) characterizes the increase of structural disorder and suggests the effectiveness of
523 the chemical exfoliation process. Due to the dependence on the number of layers of
524 graphene, G' band has been used to characterize the number of layers of graphene-based
525 nanomaterials. The inset in Figure 1f shows a 2D band for the exfoliated graphene
526 typical of few layer graphene.

527 **Figure 2a.** displays the Raman spectra of control food samples in the range of 600
528 to 3500 wavenumber region obtained using two different laser exposures of 256 and
529 512 scans, keeping the laser power constant at 150 mW. The reason for this procedure is
530 to show the consistency of the Raman data at different acquisition times. Both spectra
531 are normalized with respect to 1452 cm^{-1} band. Some of the most prominent bands
532 along with their vibrational assignment are explained as below. All the band
533 assignments were carried out using published data. The most intense Raman peak at
534 2933 cm^{-1} is assigned to the C-H stretch related to the proteins in food sample. The
535 1654 cm^{-1} is assigned to the well-known Amide I band that consists of primarily $\nu(\text{C=O})$
536 involving protein α -helix, lipids and other unsaturated fatty acids. The band around
537 1600 cm^{-1} corresponds to the Tyrosine (Tyr) signal. The Raman peak around 1450 cm^{-1}

538 is assigned to the CH₂/CH₃ deformation ($\delta(\text{CH}_2)$, $\delta_{\text{as}}(\text{CH}_3)$) involving proteins. The
539 band around 1300 cm⁻¹ is assigned to C-H deformation involving protein and lipids. The
540 peak at 1271 cm⁻¹ corresponds to Amide III band, primarily dominated by the
541 component from protein α -helix. The Raman signatures at 1122 and 1093 cm⁻¹ were
542 assigned to $\nu(\text{CC})$, $\nu(\text{CN})$ from lipids and proteins whereas the bands at 1003 cm⁻¹
543 ($\rho(\text{CH}_3)$) and 849 cm⁻¹ ($\nu(\text{CC})$) are assigned to the ring breathing mode involving
544 proteins (Gelder, 2007).

545 **Figure 2b** presents the Raman spectra of control and the food sample subjected to
546 FLG at 256 scans using 150 mW of laser power. The latter clearly shows all the
547 explained biological signatures along with the FLG marker peaks marked as asterisks:
548 G band at ~1590 cm⁻¹, D band at ~1280 cm⁻¹ and 2D band at 2560 cm⁻¹. The D and 2D
549 bands are dispersive in nature, depending on the laser excitation wavelength. The
550 unchanged position of biological markers in food sample in the presence of FLG further
551 concludes that the introduction of FLG appears to not have any significant impact on
552 the integrity of structure and composition of the components at a molecular level, and
553 can be used as an effective nondestructive biological and biomedical Raman label.

554 The biochemical analysis shows that ROS concentration was significantly
555 ($p < 0.05$) increased in gill and hepatopancreas tissues after exposure to FLG when
556 compared with the control group, while in muscle tissue this result was not observed
557 ($p > 0.05$, **Figure 3a.**).

558 Glutamate cysteine ligase (GCL) activity demonstrated a different pattern of
559 activity, as a decrease ($p < 0.05$) was observed in gill tissue while in hepatopancreas
560 tissue there was an increase in GCL activity after treatment with FLG (**Figure 3b**). In
561 muscle tissue GCL activity was unchanged in response to FLG exposure ($p > 0.05$,
562 **Figure 3b**).

563 GSH levels were increased in gill and hepatopancreas tissues in the groups
564 exposed to FLG when compared with their respective control groups ($p < 0.05$, **Figure**
565 **3c**). However, in muscle tissue this result was not observed ($p > 0.05$, **Figure 3c**).

566 The activity of GST was positively modulated in gill tissue and negatively in
567 hepatopancreas tissue ($p < 0.05$, **Figure 4a**) after FLG exposure. In muscle tissue GST
568 activity remained unchanged ($p > 0.05$, **Figure 4a**).

569 Total antioxidant capacity against peroxy radicals was increased (lower relative
570 area) in gill and hepatopancreas tissues ($p < 0.05$, **Figure 4b**) following FLG exposure,
571 while in muscle tissue this result was not observed ($p > 0.05$, **Figure 4b**).

572 In both gill and hepatopancreas tissues the treatment with dietary FLG resulted in
573 increased lipid peroxidation compared with their respective control groups ($p < 0.05$,
574 **Figure 4c**). However, no lipid peroxidation was observed in muscle tissue in response
575 to FLG exposure ($p > 0.05$, **Figure 4c**). Treatment with graphene induced DNA damage
576 in gill and hepatopancreas tissues, but not in muscle tissue, when compared with their
577 respective control groups. This increase in DNA damage in gill and hepatopancreas
578 tissues was detected with respect to the three evaluation parameters of the comet assay
579 (tail length, tail moment and % of DNA in the tail (**Figure 5a, 5b and 5c**, respectively)).
580 Histological analysis demonstrates that: normal architecture of the tissue was observed
581 in hepatopancreas tissue of the control group (**Figure 6a and 6b**), while tubule
582 deformities with light tubular alterations (LTA) were observed in the FLG group.
583 Hyperplasia of basal cells and a decrease in secretory cells (**Figure 6c**) were also
584 observed, along with hemocyte infiltrators (**Figure 6d**). No histological changes were
585 observed in both gill and muscle tissues (data not shown).

586 **5. Discussion**

587 NM possesses physical-chemical characteristics that enable their application in
588 several areas. Among NM, the carbon allotropes, such as fullerenes, nanotubes and
589 graphene are some of the most used in technology and biomedicine (Qu et al., 2013;
590 Orecchioni et al., 2014). However, with rapid development and increasing production of
591 nanotechnology, environmental contamination and specifically aquatic contamination
592 by these products is highly likely (Kahru and Doubourguier, 2010). Once into the
593 aquatic environment, NM may be dispersed in the water column and incorporated by
594 organisms and/or sediments (Koelmans et. al., 2009). Further, previous work regarding
595 NM has demonstrated the capacity of NM to be ingested by small organisms that serve
596 as food species for higher trophic levels (Baun et al., 2008). In the present study, the
597 shrimp *Litopenaeus vannamei* was used as a biological model, as it represents a
598 benthonic species widely used in aquaculture and consumed in the diet of humans
599 (Zhou et al., 2009). Although some studies have been performed evaluating the toxicity
600 of fullerene (C₆₀) and nanotubes in aquatic organisms (Canesi et al., 2010; Britto et al.,
601 2012; Da Rocha et al., 2013), few data are available regarding the effects of graphene in
602 these kinds of organisms. Evaluating the potential adverse effects of graphene in an
603 aquatic species with high commercial value such as *L. vannamei* is important to
604 understand the ecotoxicological impacts of graphene exposure.

605 Some studies have indicated that oxidative stress is a primary mechanism of
606 toxicity within CNM exposure (Britto et al., 2012; Da Rocha et al., 2013). In mammal
607 cells, exposure to graphene induced ROS production in a time and dose-dependent
608 manner with subsequent cellular apoptosis (Zhang et al., 2010). Here, an increase in
609 ROS concentration in gill and hepatopancreas tissues of shrimps was observed after 4
610 weeks of exposure to FLG (**Figure 3a**). A similar result was found in *C. elegans* after

611 exposure to graphene oxide, where an increase in ROS levels was associated with
612 physiological changes in the gut of this organism (Wu et al., 2013). The increase in
613 ROS levels after exposure to graphene and their derivatives may be related to the
614 structural form of this NM; graphenes possess a planar structure that tends to associate
615 with mitochondrial membranes, causing disruptions in the electron transport chain
616 (ETC) (Duch et. al., 2011). Zhou et al. (2014) observed alterations in electron transport
617 and subsequent decreases in ATP production in mammal cell lines exposed to graphene.
618 The ability of graphene to alter electron transport can explain the increase of ROS levels
619 observed in the present study.

620 Previous literature indicates that increases in ROS levels can induce the
621 expression of antioxidant genes, including those coding for GCL, GSH and GST. This
622 occurs through the action of the transcription factor *Nrf2*, which migrates to the nucleus
623 and interacts with antioxidant response elements (ARE) of antioxidant genes. In fact,
624 Da Rocha et al. (2013) observed up-regulation of the *Nrf2* gene following i.p. exposure
625 to single walled carbon nanotubes (SWCNT). GSH is the first line of cellular defense
626 against exposure to contaminants and oxidative damages because this tripeptide acts as
627 a scavenger of reactive species and serves as substrate for antioxidant enzymes such as
628 glutathione-S-transferase and glutathione peroxidase (GPx) (Halliwell and Gutteridge,
629 2007). In the present study, an increase in GSH content after exposure to FLG (**Figure**
630 **3c**) was observed in both gill and hepatopancreas tissue, indicating that this NM
631 induced a pro-oxidant condition that triggered an antioxidant response in these organs.

632 *De novo* GSH synthesis is related to GCL activity (White et al., 2003).
633 Interestingly, an organ-dependent response in terms of GCL activity was observed in
634 the present study. In gill tissue, GCL activity decreased, while an increase was observed
635 in hepatopancreas tissue (**Figure 3b**). Previous studies indicate that other carbon

636 nanomaterials may modulate both expression and activity of this enzyme in other
637 organisms such as freshwater fishes (Britto et al., 2012, Da Rocha et. al., 2013). As
638 GSH synthesis is an energetically expensive process, GCL activity should be regulated
639 so that enzyme activity is decreased when the reduced glutathione levels are sufficient to
640 maintain homeostasis of tissue (White et al., 2003). The increase in GSH levels
641 (approximately 4.5 fold compared with control group) observed in gills tissue may be
642 responsible for the decrease observed in GCL activity. However, in hepatopancreas
643 tissues, the increase in GCL activity induced by FLG exposure was accompanied by
644 increases in GSH content (around twice compared with control group). This result is
645 likely due to the role in metabolization/detoxification of several endogenous and
646 exogenous compounds as performed by this organ (Vogt, 1994), wherein GSH is used
647 as substrate, thus requiring high levels of this antioxidant to maintain function (about 5
648 fold higher than gills, **Figure 3c**).

649 Glutathione-S-transferase (GST) is a superfamily of enzymes involved in
650 detoxification and oxidative stress response processes, and is useful as a biomarker in
651 ecotoxicological studies (Kim et al., 2010). In fact, some studies have demonstrated that
652 GST activity is modulated in response to toxic compounds both in the gills and
653 hepatopancreas of *Litopenaeus vannamei* (Ren et al., 2015a,b). Here, an increase in
654 GST activity in gill tissue and a decrease in hepatopancreas tissue was observed
655 following FLG exposure (**Figure 4a**). Contrarily, a decrease in GST activity in gill
656 tissue of *Mytilus galloprovincialis* exposed to carbon black nanoparticles and C₆₀ was
657 observed by Canesi et al. (2010), while similar exposure induced an increase in the
658 activity of this enzyme in the digestive gland. These results suggest that each organ of
659 different species may modulate GST activity in response to different CNM. However,
660 either positive or negative modulation of GST activity represents an unfavorable

661 cellular situation, as an increase in GST activity expends GSH and leaves the tissue
662 more vulnerable to pro-oxidant conditions, while a decrease in GST activity affects the
663 detoxification capacity, allowing the accumulation of toxic compounds.

664 A similar methodology to Amado et al. (2009) was employed in the present study
665 to understand how graphene exposure can interfere in antioxidant capacity. This
666 methodology offers the advantage of evaluating total antioxidant capacity, including
667 antioxidants such as GSH. In this study, an increase in the total antioxidant capacity in
668 gill and hepatopancreas tissues was observed (**Figure 4b**). This result was expected as a
669 response to the increase in ROS levels. Further, an increase in GSH levels was observed
670 that likely significantly contributed to the observed increase in total antioxidant
671 capacity.

672 Although both gill and hepatopancreas tissues were observed to positively
673 modulate antioxidant responses in the present study, these were not sufficient to avoid
674 lipid peroxidation (**Figure 4c**). A similar result was observed in gill tissue of *C. carpio*
675 exposed to C₆₀ (Britto et al., 2012) and in mammal cells after graphene oxide exposure
676 (Chatterjee et al., 2014), suggesting that different CNM can induce oxidative damage in
677 lipids of distinct biological systems. Also, lipid peroxidation in the present study fits
678 with the observed increase in ROS levels in the same organs.

679 Although the methodology used in this study to evaluate DNA damage was not
680 specific for identifying DNA fragmentation by action of ROS, the three parameters
681 evaluated in the alkaline comet assay were in the same direction as those observed from
682 production of ROS, oxidative damage and antioxidant systems. In the present study, the
683 gill and hepatopancreas tissues of animals exposed to FLG showed more DNA damage
684 when compared to cells from unexposed animals.

685 Even though genotoxicity studies have a powerful appeal because of their close
686 relationship with mutagenesis and cancer, the number of studies is reduced when
687 compared to studies of cytotoxicity (Seabra et al., 2014). Qiao et al. (2013) investigated
688 the genotoxicity of a series of nanomaterials, observing that graphene was the most
689 harmful nanomaterial to the DNA of all the tested types. Siddique et al. (2013, 2014)
690 reported the genotoxicity of Graphene Oxide in the midgut of the fly *Drosophila*
691 *melanogaster*, even after short exposure periods (24 and 48 h). Our study reinforces the
692 genotoxicity of graphene but indicates that this action is organ-dependent.

693 Histological observations in hepatopancreas tissues showed changes such as
694 hyperplastic basal cells, infiltration of hemocytes and lower amount of secretory cells in
695 these tissues after treatment with FLG (**Figure 6b, c**) suggesting that this NM can alter
696 the structure of tissue and compromise their function. In a study by Smith and co-
697 workers (2007), several tissue disorders caused by single walled carbon nanotubes
698 (SWCNT) in liver and other tissues of the rainbow trout *Oncorhynchus mykiss*, were
699 observed, supporting evidence that CNM have the potential to induce histological
700 changes in different tissues. It is important to note that the hepatopancreas is the organ
701 responsible for metabolization and nutrition in shrimps (Sánchez-Paz et al., 2007), and
702 changes to this organ can affect detoxification capacity. In fact, GST activity in this
703 organ was severely diminished following FLG exposure (**Figure 4a**).

704

705 **6. Conclusions**

706 The results of the present study demonstrate that FLG exposure (below 2000nm
707 lateral size) induced a pro-oxidant scenario, as evidenced by an increase in ROS
708 concentration and modulations in the antioxidant system (GSH levels and GST and

709 GCL activity). Histological alterations and lipid peroxidation were observed in
710 hepatopancreas tissues of the shrimp *Litopenaeus vannamei*, characterizing an oxidative
711 stress situation. The results taken together indicate that exposure to FLG via diet may be
712 harmful to shrimps, endangering this aquatic biota. The present study offers important
713 information regarding the risks of this FLG to aquatic and environmental health,
714 especially in the context of the rapid development, production and potential
715 environmental release of these NM.

716 **Acknowledgments:** The authors would like to thank CNPq for financial support
717 (Proc. 476770/2013-0). Amanda Lucena Fernandes and Marcelo Estrella Josende are
718 graduate fellows at Coordenação de Aperfeiçoamento de Pessoal de Nível Superior
719 (CAPES). José M. Monserrat, Clascídia Furtado, Adelina Pinheiro Santos and Wilson
720 Wasielesky are research fellows at CNPq. Clascídia Furtado, Adelina Santos, Juliane
721 Ventura-Lima and José M. Monserrat are members of the Nanotoxicology Network
722 (MCTI/CNPq, Proc. 552131/2011-3).

723

724 **7. Figure captions**

725 **Figure 1.** (a), (b) and (c) Transmission electron microscopy (TEM) images of
726 graphene nanosheets obtained from diluted dispersion 1800x in NMP. (d) Histogram of
727 lateral dimensions obtained from TEM images. (e) Dynamic light scattering (DLS) of
728 graphene nanosheets dispersed in NMP. (f) Raman spectroscopy in the regions 1000-
729 4000 cm^{-1} obtained from natural graphite and graphene nanosheets. ($\lambda_{\text{exc}} = 514 \text{ nm}$, 4.6
730 mW laser power).

731 **Figure 2.** (a) FT Raman spectra of control food sample at 256 and 512 scans.
732 Laser power and spectrometer resolution were kept at 150 mW and 4 cm^{-1} respectively.
733 (b) FT Raman spectra of control (C) and graphene subjected (Gr) food samples obtained
734 using 150 mW laser power and 256 scans.

735

736 **Figure 3.** (a) Reactive oxygen species (ROS) concentration (expressed as area).
737 (b) Glutamate cysteine ligase (GCL) activity (expressed as nmol of GSH/30min/mg of
738 protein). (c) Reduced glutathione (GSH) content (expressed as μmol of GSH/mg of
739 protein). Data are expressed as the mean ± 1 standard error, n=4-5. Asterisks indicate the
740 significant difference ($p < 0.05$) to respect control group of same tissue.

741

742 **Figure 4.** (a) Glutathione-S-transferase (GST) activity (expressed as nmol of
743 CDNB conjugated/min/mg of protein). (b) Total antioxidant capacity against peroxy
744 radical (expressed as relative area). (c) Substances reactives to thiobarbituric acid
745 (TBARS) levels (expressed as nmol of MDA/mg of protein). Data are expressed as the
746 mean ± 1 standard error, n=4-5. Asterisks indicate the significant difference ($p < 0.05$) to
747 respect control group of same tissue. **CDNB:** 1-chloro-2,4-dinitrobenzene; **MDA:**
748 malondialdehyde.

749

750 **Figure 5.** DNA damage: **(a)** Tail length (in μm). **(b)** Olive tail moment. **(c)**
751 Percentage of DNA tail. Data are expressed as the mean ± 1 standard error, $n = 5$.
752 Asterisks indicate the significant difference ($p < 0.05$) to respect control group of same
753 tissue.

754

755 **Figure 6.** Histological analyzes of hepatopancreas. **(a)** and **(b)** control group,
756 arrow indicating tubular cells (TC). **(c)** Graphene group, arrow indicating hyperplasia of
757 basal cells and **(d)** Graphene group, long arrow indicating hyperplasia of basal cells and
758 short arrow indicating decrease of secretory cells and hemocyte infiltration.

759

760 **8. References**

761 Amado, L.L., Garcia, L.M, Ramos, P.B., Freitas, R.F., Zafalon, B., Ferreira, J.L.,
762 Yunes J.S, Monserrat, J.M., 2009. A method to measure total antioxidant capacity
763 against peroxy radicals in aquatic organisms: Application to evaluate microcystins
764 toxicity. *Sci Total Environ.* 407:2115-2123.

765 Baun, A., Hartmann, N.B., Grieger, K., Kusk, K.O. 2008. Ecotoxicity of
766 engineering nanoparticles to aquatic invertebrates: a brief review and recommendations
767 for future toxicity. *Ecotoxicology*, 17: 387-395.

768 Britto, R.S., Gracia, M.L., da Rocha, A.M., Flores, J.A., Pinheiro, M.V.B.,
769 Monserrat, J.M., Ferreira, J.L.R. 2012. Effects of carbon nanomaterials fullerene C₆₀
770 and fullerol C₆₀ (OH)₁₈₋₂₂ on gills fish *Cyprinus carpio* (Cyprinidae) exposed to
771 ultraviolet radiation. *Aquat Toxicol*, 114-115: 80-87.

772 Canesi, L., Fabbri, R., Gallo, G., Valloto, D., Marcomini, A., Pojano, G. 2010.
773 Biomarkers in *Mytilus galloprovincialis* exposed to suspension of selected
774 nanoparticles (Nano carbon black, C₆₀ fullerene, Nano-TiO₂, Nano-SiO₂). *Aquat*
775 *Toxicol*, 100: 168-177.

776 Chatterjee, N., Eon, H-J., Choi, J. A systems toxicology approach to the surface
777 functionality control of graphene-cells interactions. *Biomaterials*, 35: 1109-1127.

778 Da Rocha, A.M., Ferreira, J.L.R., Barros, D.M., Pereira, T.B.C., Bogo, M.R.,
779 Oliveira, S., Geraldo, V., Lacerda, R.G., Ferlauto, A.S., Ladeira, L.O., Pinheiro,
780 M.V.B., Monserrat, J.M. 2013. Gene expression and biochemical responses in brain of
781 zebrafish *Danio rerio* exposed to organic nanomaterials: Carbon nanotubes (SWCNT)
782 and fullerol (C₆₀(OH)₁₈₋₂₂(OK₄)). *Comp Biochem and Phys A*, 165: 460-467.

- 783 Duch, M.C., Budinger, G.R.S., Liang, Y.T., Soberanes, S., Urich, D., Chiarella,
784 S.E., Campochiara, M.C., Mutlu, G.M 2011. Minimizing oxidation and stable nanoscale
785 dispersion improves the biocompatibility of graphene in lungs. *NANO letters*, 11: 5201-
786 5207.
- 787 Fraser, T.W.K., Reinardy, H.C., Shaw, B.J., Henry, T.B., Handy, R.D. 2011.
788 Dietary toxicity of single-walled carbon nanotubes and fullerenes (C₆₀) in rainbow trout
789 (*Oncorhynchus mykiss*). *Nanotoxicology*, 5 (1): 98-108.
- 790 Gelder, J. D., Gussem K. D., Vandenabeele, P, Moens, L, 2007, Reference
791 database of Raman spectra of Biological molecules, *J Raman. Spectrosc*, 38, 1133-1147.
- 792 Gottschalk, F., Sonderer, T., Scholz, R.W. 2009. Modeled environmental
793 concentration of engineered nanomaterials (TiO₂, ZnO, Ag, CNT, fullerenes) of
794 different regions. *Environ Sci and Technol*, 43: 9216-9222.
- 795 Habig, W.H., Pabst, M.J., Jakoby, W.B., 1974. Glutathione-S-transferases: The
796 first enzymatic step in mercapturic acid formation. *J Bioll Chem*, 249: 7130-7139.
- 797 Halliwell, B., Gutteridge, J.M.C. 2007. Free radicals in Biology and Medicine.
798 Oxford University Press Inc, New York. 851.
- 799 Handy, R.D., Al-Bairuty, G., Al-Jubory, A., Ramsden, C.S., Boyle, D., Shaw,
800 B.J., Henry, T.B. 2011. Effects of manufactured nanomaterials on fishes: a target organ
801 and body system physiology approach. *J Fish Biol*, 79(4): 821-53.
- 802 Kahru, A., Dubourguier, H-C. 2010. From Ecotoxicology to Nanoecotoxicology.
803 *Toxicology*, 105-119.

- 804 Khan, U., Porwal, H., O'Neill, A., Nawaz, K., May, P., Coleman, J. N. 2011.
805 Solvent-Exfoliated Graphene at Extremely High Concentration. *Langmuir*, 17: 9077–
806 9082.
- 807 Kim, I.H., Dahms, H.V., Rhee, J.S., Lee, Y.M., Lee, J., Han, K.N., Lee, J.S. 2010.
808 Expression profile of seven glutathione-S-transferase (GST) genes in cadmium-exposed
809 river pufferfish (*Takifugu obscurus*). *Comp Biochem and Phys C*, 151: 99-106.
- 810 Koelmans, A.A., Nowach, B., Wiesner, M.R. 2009. Comparison of manufactured
811 and black carbon nanoparticle concentration in aquatic sediments. *Environ Pollut*, 157:
812 1110-1116.
- 813 Lobato, R.O., Nunes, S.M., Wasielesky, W., Fattorini, D., Regoli, F., Monserrat,
814 J.M., Ventura-Lima, J. 2013. The role of lipoic acid in the protection of metallic
815 pollutant effect in the shrimp *Litopenaeus vannamei* (Crustacea, Decapoda). *Comp*
816 *Biochem and Phys A*, 165: 491-496.
- 817 Lotya, M., Rakovich, A., Donegan, J.F., Coleman, J.N. 2013. Measuring the
818 lateral size of liquid-exfoliated nanosheets with dynamic light scattering.
819 *Nanotechnology*, 24: 265703.
- 820 Matranga, V., Corsi, J. 2012. Toxic effect of engineered nanoparticles in the
821 marine environment: model organisms and molecular approach. *Mar Environ Res*, 76,
822 32-40.
- 823 Oakes, K.D., Kraak, G.J.V., 2003. Utility of the TBARS assay in detecting
824 oxidative stress in white sucker (*Catostomus commersoni*) populations exposed to pulp
825 mill effluent. *Aquat Toxicol*, 63: 447-460.

- 826 Orecchini, M., Bedognitti, D., Sgavolla, F., Marencola, F.M., Bianco, A., Delogu,
827 L.G. 2014. Impact of carbon nanotubes and graphene on immune cells. *J Trans Med*,
828 *12:138*.
- 829 Powell, J.J., Faria, N., Thomas-Mckay, E., Pele, L.C. 2010. Origin and fate of
830 dietary nanoparticles and microparticles in the gastrointestinal tract. *J Autoimmun*, 34:
831 J226-J233.
- 832 Pretti, C., Oliva, M., Di Pietro, R., Monni, G., Cevasco, G., Chiellini, F., Pomelli,
833 C., Chiape, C. 2014. Ecotoxicity of pristine graphene to marine organisms. *Ecotox*
834 *Environ safe, 101: 138-145*.
- 835 Qiao, Y., An, J., Ma, L. 2013. Single cell array based assay for *in vitro*
836 genotoxicity study of nanomaterials. *Anal Chem*, 85: 4107-4112.
- 837 Qu, X., Brame, J., Li, Q., Alvarez, P.J.J. 2013. Nanotechnology for a safe and
838 sustainable water supply: Enabling integrated water treatment and reuse. *Accounts*
839 *Chem Res*, 46: 834-843.
- 840 Ren, X., Pan, L., Wang, L. 2015 (a). The detoxification process, bioaccumulation
841 and damage effect in juvenile white shrimp *Litopenaeus vannamei* exposed to crysene.
842 *Ecotox Environ Safe, 114: 44-51*.
- 843 Ren, X., Pan, L., Wang, L. 2015 (b). Toxic effect upon exposure to
844 benzo(a)pirene in juvenile white shrimp *Litopenaeus vannamei*. *Environ Toxicol and*
845 *Phar, 39: 194-207*.
- 846 Sánchez-Paz, A., Garcia-Carreño, F., Hernández-López, J., Muhlia-Almazán, A.,
847 Yepiz-Plascencia, G. 2007. Effect of short-term starvation on hepatopancreas and

848 plasma energy reserves of the Pacific white shrimp (*Litopenaeus vannamei*). *Journal of*
849 *Exp Mar Biol Ecol*, 340: 184-193.

850 Seabra, L.M.J., Damasceno, K.S.F.S.C., Silva, C.R., Gomes, C.C., Pedrosa,
851 L.F.C. 2014. Total carotenoids in white shrimp (*Litopenaeus vannamei*) waste. *Rev.*
852 *Ceres*, Viçosa, v. 61: 130-133.

853 Siddique, Y.H., Fatima, A., Jyoti, S., Naz, F., Rahul, Khan, W., Singh, B.R.,
854 Navqi, A.H. 2013. Evaluation of the Toxic Potential of Graphene Copper
855 Nanocomposite (GCNC) in the Third Instar Larvae of Transgenic *Drosophila*
856 *melanogaster* (hsp70-lacZ)Bg9. *PLoS ONE* 8 (12): e80944.

857 Siddique, Y.H., Khan, W., Khanam, S., Jyoti, S., Naz, F., Rahul, Singh, B.R.,
858 Navqi, A.H. 2014. Toxic potential of synthesized graphene zinc oxide nanocomposite in
859 the third instar larvae of transgenic *Drosophila melanogaster* (hsp70-lacZ) B g9.
860 *BioMed Res Inter*.

861 Singh, S. K., Devi, A. A., 1998. Effect of grasses fed to pigs by different methods
862 on their growth rate and feed conversion efficiency. *Indian J. Anim. Sci.*, 68 (7): 693-
863 695.

864 Smith, C., Shaw, B., Handy, R. 2007. Toxicity of single walled carbon nanotubes
865 on rainbow trout, (*Onchorhyncos mykiss*): Respiratory toxicity, organ pathologies, and
866 other physiological effects. *Aquat Toxicol*, 82, 94-109.

867 Viarengo, A., Burlando, B., Cavaletto, M., Marchi, B., Panzano, E., Blasco, J.,
868 1999. Role of metallothionein against oxidative stress in the mussel *Mytilus*
869 *galloprovincialis*. *Am J Physiol*, 46: 1612-1619.

870 Vogt, G. 1994. Life-cycle and functional cytology of the hepatopancreas cells of
871 *Astacus* (Crustacea, Decapoda). *Zoomorphology* 114, 83–101.

872 White, C.C, Viernes, H., Krejsa, C.M., Botta, D., Kavanagh, T.J., 2003.
873 Fluorescence-based microtiter plate assay for glutamate-cysteine ligase activity. *Anal*
874 *Biochem*, 318: 175-180.

875 Waisse-Leinonen, G.C., Petersen, G.C., Pakarinen, K., Akkanen, J., Leppänen,
876 M.T., Kukkonen, V.K. 2012. Toxicity of fullerene (C₆₀) to sediment-dwelling
877 invertebrate *Chironomus riparius* larvae. *Environ Toxicol Chem*, 31: 2108-2116.

878 Wu, Q., Yin, L., Li, X., Tang, M., Zhang, T., Wang, D. 2013. Contribution of
879 altered permeability of intestinal barrier and defecation behavior to toxicity formation
880 from graphene oxide in nematode *Caenorhabditis elegans*, *Nanoscale*, 5: 9934-9943.

881 Zar, J.H. 1984. Biostatistical analysis. New Jersey, Ed. Prentice Hall. 718pp.

882 Zhang R, Niu Y, Li Y, Zhao C, Song B, Li Y, Zhou Y . 2010. Acute toxicity study
883 of the interaction between titanium dioxide nanoparticles and lead acetate in mice.
884 *Environ Toxicol Pharm*, 30:52–60. doi:10.1016/j.etap.2010.03.015

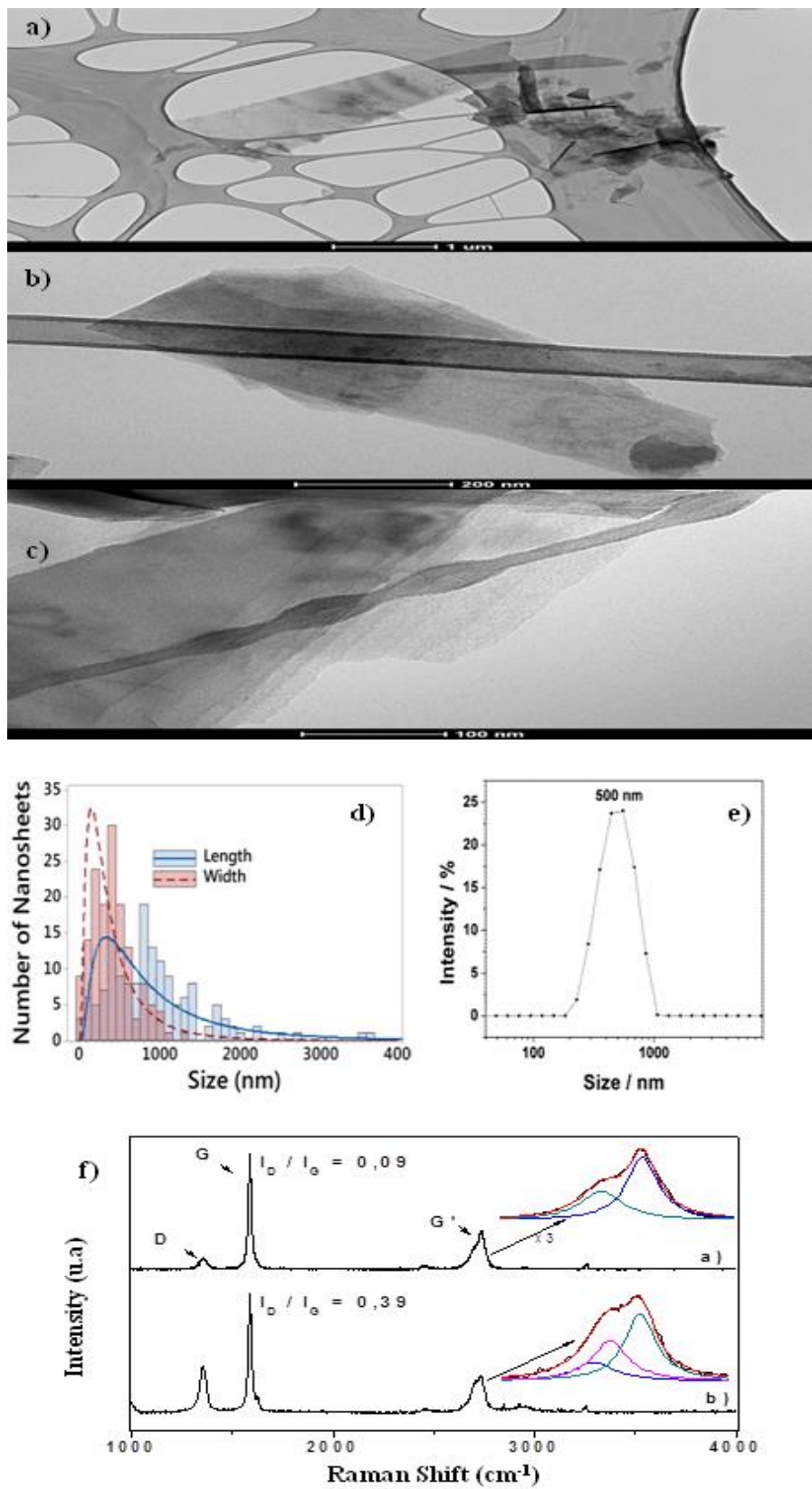
885 Zhang, X., Yin, J., Peng, C., Hu, W., Zhu, Z., Li, W., Fan, C., Huang, Q. 2011.
886 Distribution and biocompatibility studies of graphene oxide in mice after intravenous
887 administration. *Carbon*, 99: 986-995.

888 Zhou, J., Wang, W-N., Wang, A-L., He, W-Y., Zhou, Q-T., Liu, Y., Xu, J. 2009.
889 Glutathione S-transferase in the white shrimp *Litopenaeus vannamei*: Characterization
890 and regulation under pH stress. *Comp Biochem Phys C*, 150:224–230.

- 891 Zhou, H., Zhang, B., Zheng, J., Yu, M., Zhou, T., Zhao, K., Jia, Y., Gao, X.,
892 Chen, C., Wei, T. 2014. The inhibition and migration of invasion of cancer cells by
893 graphene via the impairment of mitochondrial respiration. *Biomaterials*, 35: 1597-15
- 894 Zhu, X., Wang, J., Zhang, X., Chang, Y., Chen, Y. 2010. Trophic transfer of TiO₂
895 nanoparticles from daphnia to zebrafish in a simplified freshwater food chain.
896 *Chemosphere*, 79: 928-933.
- 897 Wang, L., Wang, X-R., Liu, J., Chen, C-X., Liu, Y., Wang, W-N. 2015. Rab from
898 the white shrimp *Litopenaeus vannamei*: characterization and its regulation upon
899 environmental stress. *Ecotoxicology*, DOI 10.1007/s10646-015-1481-1.
- 900 Wu, Q.L., Yin, L., Li, X., Tang, M., Zhang, T., and Wang, D.T., 2013.
901 Contributions of altered permeability of intestinal barrier and defecation behavior to
902 toxicity formation from graphene oxide in nematode *Caenorhabditis elegans*.
903 *Nanoscale*; 5: 9934-9943.

904

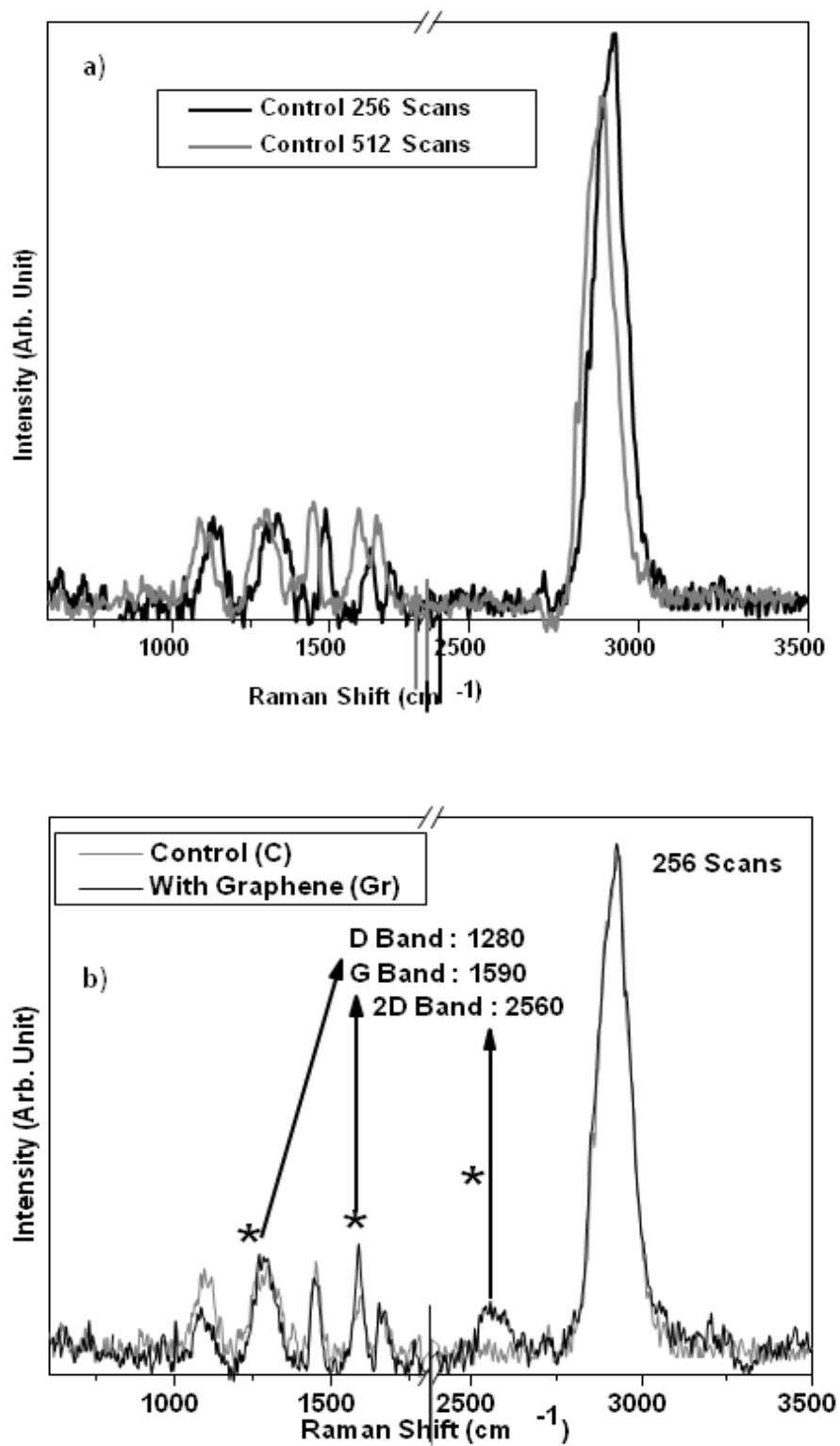
9. Figures



905

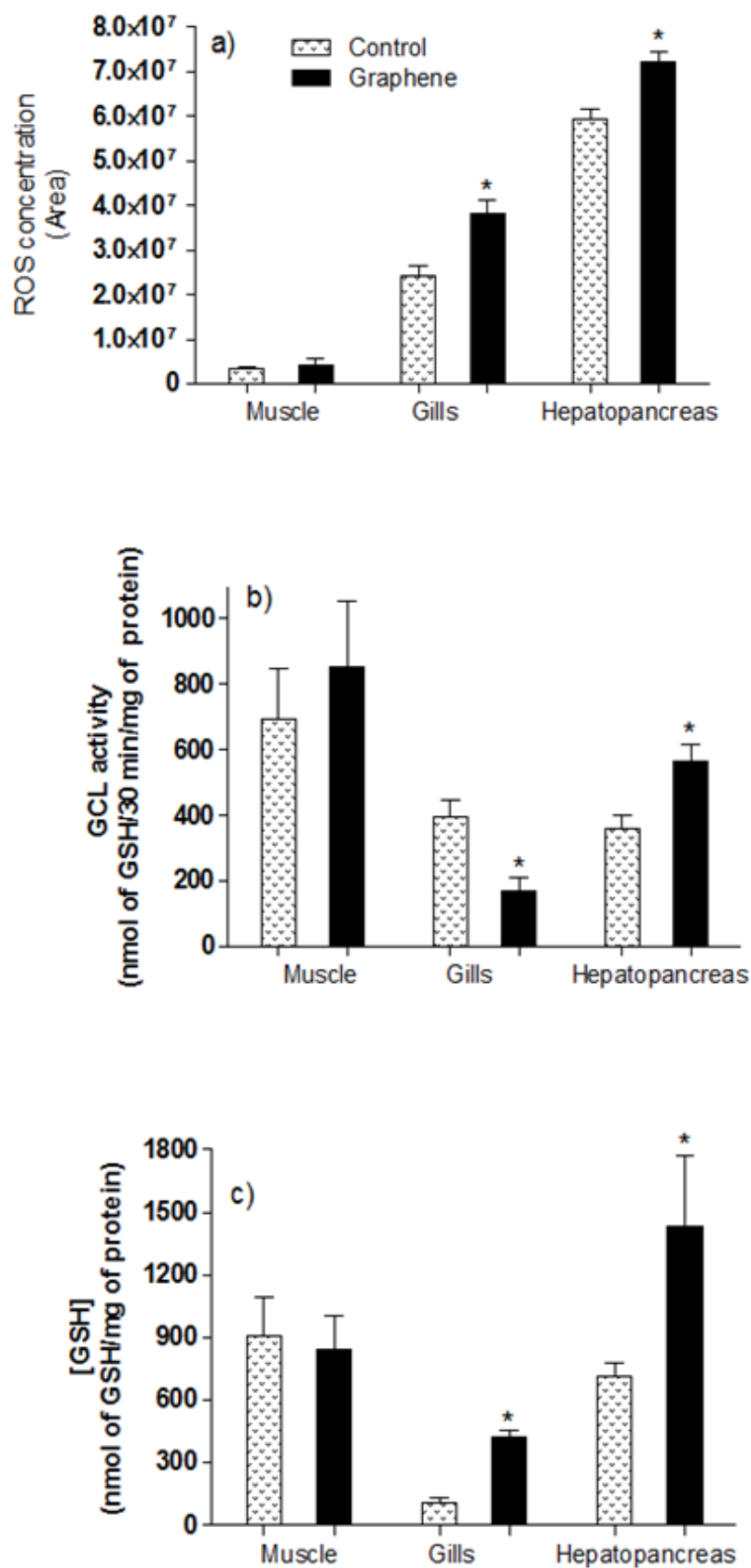
906

Figure 1.



907

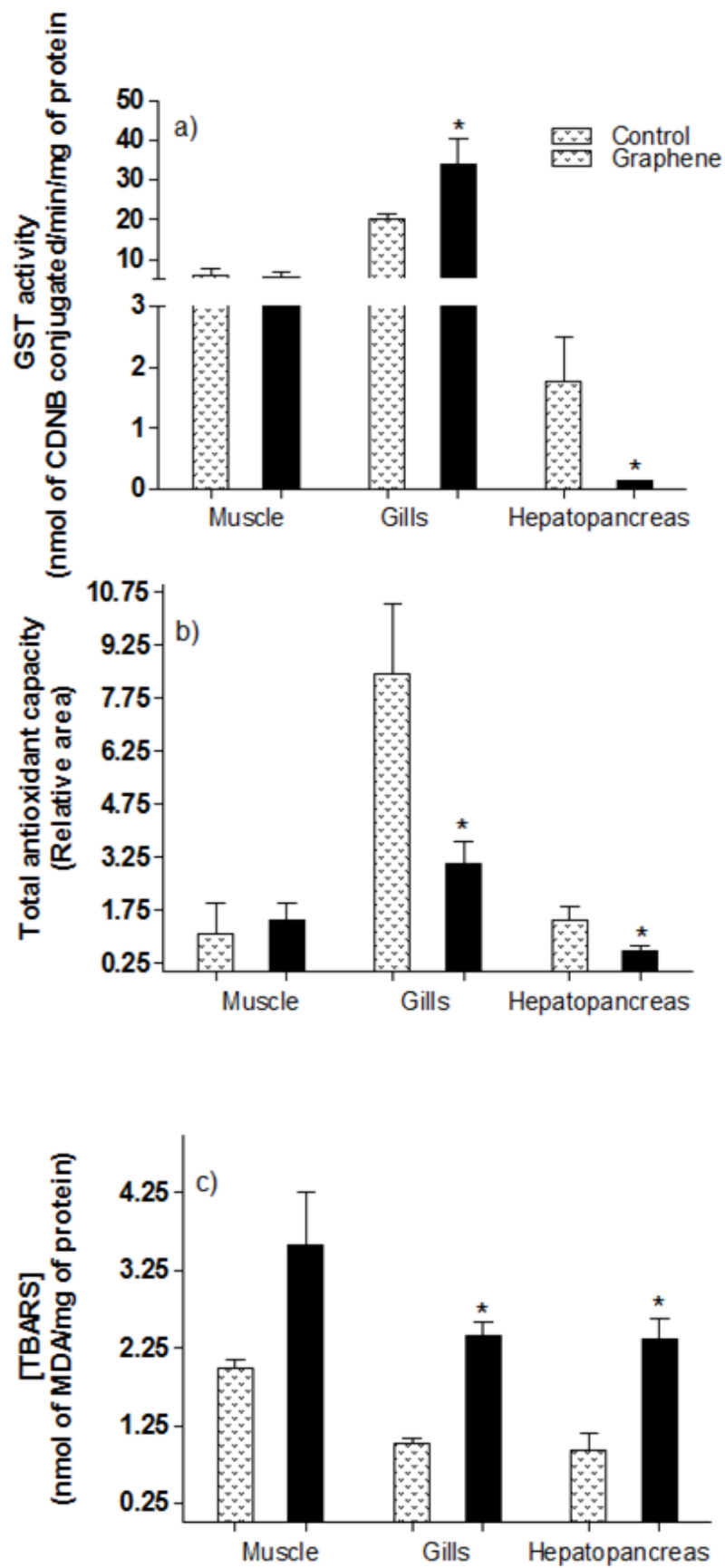
908 **Figure 2.**



909

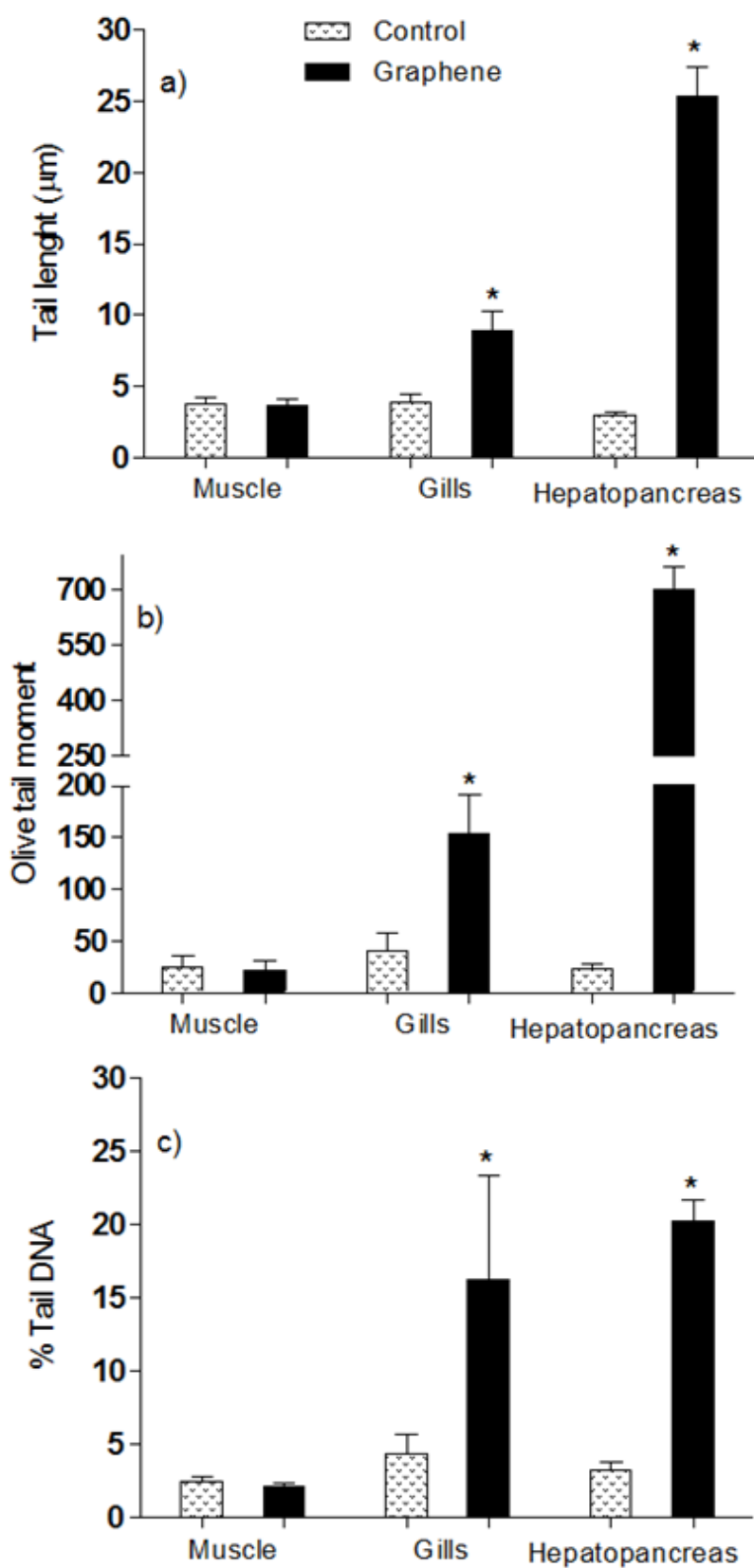
910

Figure 3.



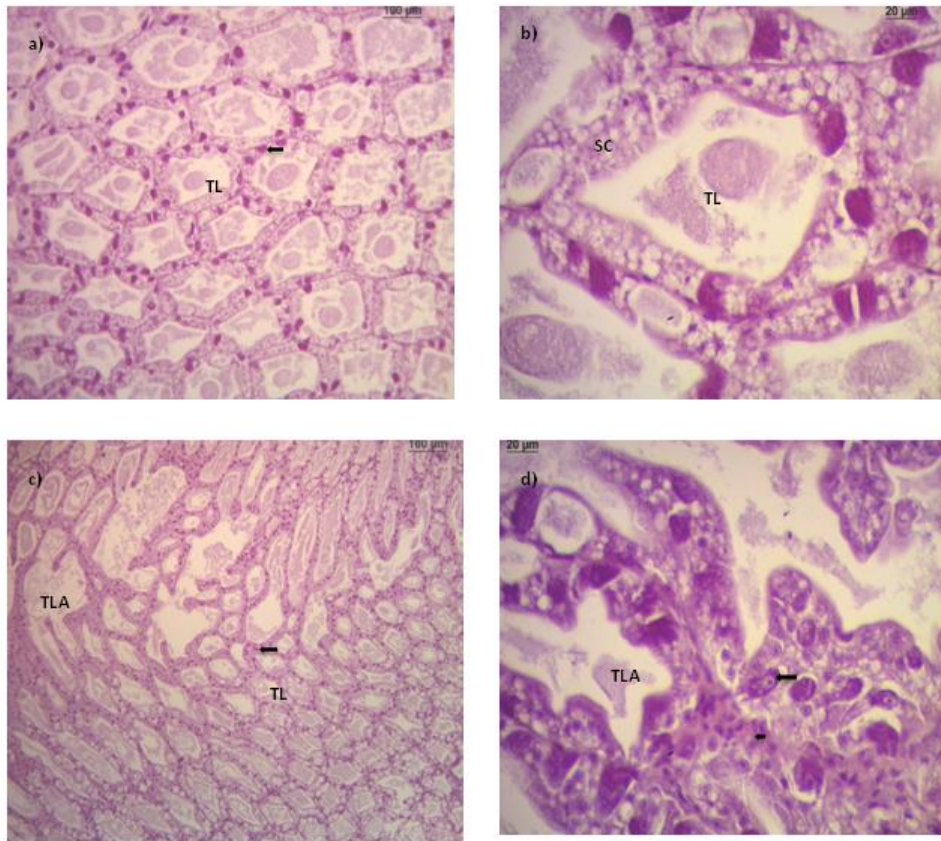
911

912 **Figure 4.**



913

914 **Figure 5.**



915

916 **Figure 6.**

917

6. Capítulo 2

Evaluation of graphene effects in different tissues of *Danio rerio* (Cyprinidae): a molecular, biochemical and histological approach.

To be submitted to Comparative Biochemistry and Physiology, part C

Amanda Lucena Fernandes^{1,2*}, Jefferson Patrício Nascimento³, Adelina Pinheiro Santos³, Carlos Eduardo da Rosa^{1,2}, Luis Alberto Romano⁴, Clascídia Aparecida Furtado³, José Marià Monserrat^{1,2,4},
Juliane Ventura-Lima^{1,2*}.

¹Instituto de Ciências Biológicas (ICB), Universidade Federal do Rio Grande - FURG, Rio Grande, RS, Brasil.

²Programa de Pós-Graduação em Ciências Fisiológicas - FURG.

³Centro de Desenvolvimento da Tecnologia Nuclear – CDTN/CNEN, Belo Horizonte, MG, Brazil.

⁴Programa de Pós-Graduação em Aquicultura-FURG.

* Corresponding authors: Amanda Lucena Fernandes (E-mail:

amandalfernandes@outlook.com)

Juliane Ventura-Lima (E-mail: juliane_ventura@yahoo.com.br).

918 **Abstract**

919 The use of graphene increased in the last years, leading to a higher chance of
920 being released into the environment and coming into contact with organisms. Data on
921 graphene toxicology has shown its ability to alter the antioxidant system and cause
922 oxidative stress in marine crustaceans; however, information regarding fish toxic
923 effects data is scarce. Based on this, the aims of this study was to evaluate the effects
924 of graphene in different tissues of the *Danio rerio* fish, evaluating parameters of
925 oxidative stress. Animals were exposed intraperitoneally (*i.p*) to 10 ul of two
926 concentrations of graphene, 5 and 50 mg/L during 48 h, after they were euthanized
927 and gills, intestine, muscle and brain dissected. It was analyzed parameters of
928 oxidative stress, as expression of the *nrf2* and *gclc* genes, as well as the activity of the
929 GCL (glutamate cysteine ligase) enzyme, reduced glutathione (GSH) concentration,
930 glutathione-S-transferase (GST) activity and lipid peroxides levels. Histological
931 analyses were also performed to observe if the exposure can induce pathological
932 damage in different tissues. Results showed no significant difference in the expression
933 of *gclc* and *nrf2* genes after the exposure. In contrast GCL and GST activity and GSH
934 concentration were affected regarding SDS-control, in different tissues and different
935 concentrations. Lipid damage was observed in gills, also pathological damage was
936 observed after the exposure of both concentrations, excluding intestine. Overall,
937 results indicated that graphene induced toxicological effects that depend of the
938 analyzed organ, causing distinct pathologic effects on some, and oxidative effects on
939 others.

940 **Key-words:** antioxidant system, carbon nanomaterials, nanotoxicology, *Danio rerio*,
941 oxidative stress.

942 ¹ **Abbreviations:**

943

¹ CNM, carbon nanomaterials; *i.p*, intraperitoneal; GCL, glutamate-cysteine-ligase; GSH, reduced glutathione; GST, glutathione-S-transferase; GR, graphene; MWCNT, multi-walled carbon nanotubes; SWCNT, single walled carbon nanotubes; NM, nanomaterials; *nrf2*, Nuclear factor [erythroid-derived 2]-like 2; PEG, peglated; SDS, sodium dodecyl sulphate.

944 1. Introduction

945 Graphene (GR) is a nanomaterial (NM) consisting of a single layer of carbon
946 atoms with two dimensions and a one-sheet structure (nanosheets) (Mafra, 2008). Its
947 several properties include the high electrical conductivity, thermal and chemical
948 stability, as well as its large surface area. Due these characteristics, an increased the use
949 of NM has been registered in different areas of sciences (Chen et al., 2010; Huang and
950 Shi, 2012, Nguyen and Berry, 2012). Besides, graphene is resistant to degradation due
951 to its large surface/volume ratio and morphology, because both its surface and its edges
952 are electric active, and are great sites for the attraction of biological molecules, being so
953 endangering for living organisms (Stankovich et al., 2006, Yang et al., 2013).

954 Among the effects caused by GR exposure it can be highlighted cellular
955 membrane agglutination, induction of oxidative stress in some cell types of bacteria and
956 mammals (Jaworski et al., 2013, Li et al., 2012, Markovic et al., 2011, Nguyen and
957 Berry, 2012, Zhang et al., 2010). In different marine crustacean (*Artemia salina* and
958 *Litopenaeus vannamei*) the *in vivo* exposure to graphene induced antioxidant responses
959 and oxidative damages to macromolecules, characterizing an oxidative stress situation
960 (Pretti et al., 2014; Fernandes et al., 2017).

961 Until now, data about effect of GR exposure in fishes are scarce (Yang et al.,
962 2013). For this reason, in this study, *Danio rerio* was the selected biological model,
963 being an organism commonly used in scientific studies due to specific characteristics
964 such as rapid development, small size, low production cost and its already unveiled
965 genome (Lawrence, 2007). The species is also a model for toxicity studies for display
966 biochemical, molecular, and behavioral responses to different types of NM (Da Rocha
967 et al., 2013, Filho et al., 2014, Webber et al., 2014).

968 In this way, the objective of this study was to analyze toxic effects of GR
969 considering molecular and biochemical responses of oxidative stress, and histological
970 alterations in different organs of zebrafish *Danio rerio*, caused by GR intraperitoneal
971 (*i.p*) exposure. This exposure route (*i.p*) was chosen to assure that the animals receive a
972 precise dose of this NM, since it is known that oral absorption of peglated graphene by
973 the intestine is limited in mammals, so *i.p* exposure would be more appropriate in
974 experiments (Yang et al., 2013). Previous studies have employed the same approach to
975 analyze the toxic effects induced by carbon nanomaterials in zebrafish (da Rocha et al.,
976 2013). The data obtained in this study, will certainly contribute to know part of toxic
977 effect induced by graphene in fishes and to infer in other species that possess molecular
978 similarity with *D. rerio*.

979 **2. Material and Methods**

980 **2.1 Biological model and maintenance of animals**

981 Animals were obtained from a local supplier and kept in the aquarium of the
982 Biological Sciences Institute (ICB) of the Federal University of Rio Grande (FURG) for
983 acclimatization for at least two weeks prior experiments in 60 L aquariums (maximum
984 of 100 animals per aquarium). They were kept under photoperiod conditions 12 hours
985 light/12 hours dark, temperature 28 °C, pH 7.5-8.0, and constant aeration with feed
986 twice a day.

987 **2.2 Obtainment and characterization of graphene**

988 Graphene was obtained in procedure of two steps, first 3.3 g of natural graphite
989 (Graflake 99580-supplied from Nacional do Grafite LTDA-Brazil) was added in 1.000
990 ml of NMP (1-methyl-2-pyrrolidinone, Sigma-Aldrich) and after, it was submitted to
991 ultrasonic bath for 168h and centrifuged at 110 x g during 45 min. The supernatant
992 then was filtered in a nylon membrane (0.2 µm of diameter), washed with 400 ml

993 deionized water, 200 ml of ethanol (95% P.A) and 100 ml of diethyl ether (Synth P.A)
994 and dried during 24 h at 150 °C under vacuum. Secondly, it was added 16 ml of NMP
995 (24 mg.mL⁻¹) and sonicated during 24 h, after, the dispersion obtained was kept
996 standing during 8 days and the supernatant was collected and filtered. Finally the
997 material was washed and dried as described above. This methodology is based on Khan
998 et al. (2011).

999 In this study was used the same sample of graphene utilized in our previous
1000 work and a broad characterization of nanomaterial was performed and described in the
1001 mentioned study (Fernandes et al., 2017).

1002 **2.3 Preparation of the solution with graphene**

1003 Two graphene solutions were prepared, one of 5 and other of 50 mg of
1004 graphene/L, the different concentrations (low and high) were chose to observe if the
1005 graphene would agglomerate and cause different effects. The concentrations chosen was
1006 based on Fernandes et al. (2017), being chosen one 10 times lower (50mg) and other
1007 lowest (5mg). The detergent sodium dodecyl sulphate (SDS) (3 g/L) was used as
1008 vehicle; SDS was diluted in MilliQ water, after graphene was added to that solution and
1009 then sonicated (ECO SONICS - Ultrasonique, 40kHz, 150VA) during 5 h. This
1010 methodology was based on Da Rocha et al. (2013) and Smith et al. (2007).

1011 **2.4 Graphene exposure**

1012 The graphene solution was administered intraperitoneally (*i.p*) for this, the
1013 animals were anesthetized by immersion on tricaine (MS-222) for about 1minute, then
1014 10 µl of solution (graphene or vehicle) were injected into the animal. After, there were
1015 placed in a beaker with oxygenated clean water for recovery that occurred between 30 s
1016 and 1 min (Da Rocha et al. 2013). Animals were not fed 24 h prior or during the

1017 experiment, and after 48 h fish were euthanized by immersion on 500 mg/L of tricaine,
1018 and gills, intestine, muscle and brain were removed.

1019 Experimental design consist on: Animals were divided in four groups and pool
1020 of six fish was used to compose one sample (n=5-6 pools) in biochemical analysis,
1021 while for molecular analysis it was chosen a pool of three fishes; animals were exposed
1022 twice intraperitoneally in 48 h: one exposure at 0h and the other 24h after, to their due
1023 treatments, being killed after 48 hours of exposure. All procedures performed in this
1024 study were in accordance with the EU Directive 2010/63/EU for animal experiments.
1025 Experimental groups are described below:

1026 Control-control group: Animals were kept in aquarium and after period of
1027 acclimatization received *i.p.* of 10 µl MilliQ water.

1028 SDS-control group: After acclimatization the animals received *i.p.* of 10 µl of
1029 SDS detergent. SDS group was used as a second control, besides MilliQ water, because
1030 the graphene was dispersed in SDS solution, so it was tested if the detergent alone
1031 induced a toxic response.

1032 Graphene group 1 (G1) - low concentration: After acclimatization period
1033 animals received *i.p.* of 10 µl of graphene solution of 5 mg/L.

1034 Graphene group 2 (G2) - high concentration: After acclimatization period
1035 animals received *i.p.* of 10 µl of graphene solution in concentration of 50 mg/L.

1036 This form of exposure has been selected to ensure that the animal is exposed to
1037 an exact concentration of graphene since when dispersed in water the characteristics of
1038 the nanomaterial can form agglomerate altering the size of the NM and possibly their
1039 the biological effects. The use of all animals in this experiment was approved by the
1040 Ethics Committee for Experimental Animal Use (CEUA) from Universidade Federal do
1041 Rio Grande (FURG), through the process number 23116001258/2015-16.

1042 **2.6 Gene expression**

1043 In order to analyze glutamate-cysteine-ligase catalytic subunit (*gclc*) and
1044 Nuclear factor [erythroid-derived 2]-like 2 (*nrf2*) genes expression, Real-time PCR were
1045 performed in samples of gills, intestine and muscle (based on Rosa *et al.* 2010. Briefly,
1046 after dissection the tissues were immediately immersed in TRIzol® reagent (Invitrogen,
1047 USA) for the extraction of total RNA according the manufacturer's instructions.
1048 Afterwards, RNA concentration was quantified by spectrophotometry (280 and 260nm),
1049 and integrity was checked using agarose gel (1%) electrophoresis. Sequentially,
1050 complementary DNA (cDNA) was prepared from the total RNA, using High Capacity
1051 cDNA Reverse Transcription Kit (Applied Biosystems) and used as a template for the
1052 amplification of *gclc* and *nrf2* genes, the specific primers are escribed in **Table 1**. The
1053 PCR reactions were performed on the Applied Biosystems 7300 Sequence Detection
1054 System, using the SYBR-Green PCR Master Mix (Applied Biosystems). The
1055 housekeeping genes *ef1a* (elongation factor 1 alpha) and *18S* (ribosomal RNA) were
1056 employed to normalize the *gclc* and *nrf2* expression in the tissues. Brains were not used
1057 to this analysis due to lack of tissue sample. The data were analyzed by the deltadelta
1058 CT method and the results expressed as relative gene expression considering the SDS-
1059 control group gene expression as 1.

1060 **2.7 Biochemical analysis**

1061 **2.7.1 Preparation of homogenates**

1062 Gills, intestine, muscle and brain of *D. rerio* were homogenized (1:5; p/v) in
1063 homogenization buffer containing Tris-HCl (100 nM, pH7.75), EDTA (2 mM) and
1064 Mg²⁺ (5 mM) (Da Rocha et al., 2013). The homogenates were centrifuged at 10,000 *x g*
1065 for 20 minutes at 4°C and the supernatants were used for the dosages of the enzymatic

1066 activities, the total proteins were quantified using a commercial kit based on Biuret
1067 method using a microplate reader (BiotekELx 800) at 550nm.

1068 **2.7.2 Enzymatic assays**

1069 To determine the GCL activity and GSH levels was employed the methodology
1070 described by White et al. (2003). This analyze is based on the ability of the compound
1071 2,3-naphtalenedicarboxaldehyde (NDA) to react with γ -glutamylcysteine (γ -GC) and/or
1072 glutathione (GSH) forming a fluorescent cyclic compound (GC-NDA and GS-NDA,
1073 respectively). The fluorescence of this complexes were measured on a fluorometer (2
1074 Victor, Perkin Elmer) with wavelengths of 485 and 535 nm for excitation and emission,
1075 respectively.

1076 Glutathione-S-transferase (GST) activity consist on the analysis of using
1077 absorbance for evaluate the conjugation of 1 mM GSH (Sigma) with 1 mM of the
1078 reagent 1-chloro-2,4-dinitrobenzene (CDNB, Sigma), a reaction catalyzed by GST. The
1079 complex formed has a maximum absorbance at 340 nm. Methodology was determined
1080 according to Habig et al. (1974).

1081 The lipid peroxidation was measured by fluorimetry of thiobarbituric acid
1082 reactive substance (TBARS) method (Oakes and Kraak 2003). The method is involves
1083 reagents like tetramethoxypropane (TMP, Sigma), and is based on a reaction of
1084 malondialdehyde (MDA), a degradation product of peroxidized lipids, with thiobarbituric
1085 acid (TBA) under conditions of high temperature and acidity, resulting in a fluorescent
1086 chromogen detected in wavelength of 595 nm (emission) and 520 nm (excitation). The
1087 content of lipid peroxide was expressed as nmol of TBARS/mg of protein.

1088 **2.8 Histological analysis**

1089 The fish were euthanized (n=6) and after a cuts were made sectioning head and
1090 part of the fishes muscle leaving the entrails exposed to the fixative, after whole fish
1091 were put in cassetts and fixed in 10% buffered formalin (10% formaldehyde, 90%
1092 distilled water, dibasic sodium phosphate 6.5g, monobasic sodium phosphate 4.0g) for
1093 histopathological evaluation. Samples were processed in an automatic tissues processor
1094 LUPE PT 05 (dehydration, rinsing, clearing and impregnation) and put in Paraplast
1095 (Sigma-Aldrich), after the tissues were sectioned in microtome (LUPETEC MRPO3) at
1096 4µm sections. The sections were stained with hematoxylin and eosin (H&E), after
1097 staining the slides were dehydrated during 3 min in 70, 80, 90 and 96% ethanol, rinsed
1098 twice in ethanol 100% for 5 min and cleared with xylene.

1099 **3. Statistical analysis**

1100 The statistical differences were tested using one-way variance analysis
1101 (ANOVA) follow by Neuman-Keuls test as *post hoc* comparison, significance level was
1102 fixed in 5%, the normality and variance were previously checked and mathematical
1103 transformations were made when necessary (Zar, 1984).

1104 **4. Results**

1105 TEM images showed that some graphene nanosheets were agglomerated, but the
1106 majority possessed well-defined borders, approximately 10 layers of graphene and
1107 distribution of lateral sizes between 100 and 2000 nm with average value of length and
1108 width of 900 and 400 nm, respectively (**Figure 1**).

1109 Considering the glutamate cysteine ligase catalytic subunit gene expression
1110 (*gclc*) no effects were observed in gills, intestine and muscle after the animal being
1111 exposed to the two graphene solutions ($p>0.05$; **Figure 2a, 2b** and **2c**, respectively).
1112 Same results were obtained for *nrf2* expression (**Figure 3**; $p>0.05$).

1113 The GSH concentration decreased after the exposure of G1 in gills compared to
1114 SDS-Control group ($p < 0.05$; **Figure 4a**), the same was not observed in intestine, that
1115 showed an increased concentration in G1 when compared to SDS-control group
1116 ($p < 0.05$; **Figure 4b**). In muscle the exposure does not seem to had any effect ($p > 0.05$;
1117 **Figure 4c**), while in brain, both G1 and G2 showed an increase in concentration
1118 compared to SDS-control ($p < 0.05$; **Figure 4d**).

1119 Glutamate-cysteine-ligase activity was not modulated in gills ($p > 0.05$; **Figure**
1120 **5a**), while intestine showed an increase of activity in G1 and G2 when compared to
1121 SDS-control ($p < 0.05$; **Figure 5b**). In muscle, it was not observed any difference
1122 between groups ($p > 0.05$; **Figure 5c**), as for brain an increase of activity in G1 and G2 it
1123 was observed when compared with SDS-control ($p < 0.05$; **Figure 5d**).

1124 GST activity remains almost constant in gills ($p > 0.05$, **Figure 6a**). A different
1125 result was observed in intestine, where the treatment with graphene on low dose induced
1126 an increase on the activity of GST when compared to SDS-control group ($p < 0.05$,
1127 **Figure 6b**). In muscle no modulation of the enzyme activity was observed ($p > 0.05$,
1128 **Figure 6c**). In brain, was observed that G1 induced an increase in this enzyme activity
1129 when compared to SDS-control ($p < 0.05$, **Figure 6d**).

1130 In gills it was observed an increase in lipid peroxidation in the group exposed to
1131 higher concentration of graphene (G2) when compared to SDS-control group ($p < 0.05$,
1132 **Figure 7a**). A different result was observed in intestine and brain, where lipid damage
1133 was not observed after exposure to both graphene concentrations ($p > 0.05$, **Figure 7b**
1134 and **7d** respectively). In muscle, both graphene concentrations showed to decrease the
1135 lipid damage levels when compared with SDS-control group ($p < 0.05$, **Figure 7c**).

1136 Histological changes were observed in gills, where cells suffered moderate and
1137 severe hyperplasia after the exposure to G1 and G2, respectively (**Figure 8a**). While in
1138 the intestine, it was not observed any tissue alterations for the different treatments
1139 (**Figure 8b**). Besides, the muscle suffered pathological damage, being observed
1140 inflammatory infiltrates between the muscular fibers in the two groups of graphene-
1141 exposed fish (**Figure 8c**). Brain showed that exposure to G1 caused ganglionic
1142 proliferations, increased microglia cells and moderate edema, while exposure to G2
1143 increased the ganglionic proliferation leading to a larger number of astrocytes, and
1144 caused severe edema (**Figure 8d**).

1145 **5. Discussion**

1146 The use of NM, including carbon nanomaterials, had increased constantly for
1147 over the last years, due to its unique physical and chemical characteristics that allow
1148 them to be implemented in multiples scientific fields, such as biological and
1149 pharmaceutical as well as technological (Aitken et al., 2006, Oberdörster, 2004). The
1150 release of NM into aquatic environment is an important aspect to be considered, so that
1151 it is possible to evaluate the damage for the present species in this environment, that are
1152 probably being exposed to toxic effects through inhalation and/or direct contact with
1153 these nanomaterials (Park et al., 2011, Zhang et al., 2011). It was already demonstrated
1154 that GR and GO are capable of inducing oxidative stress in others aquatic species, such
1155 as the crustacean *Litopenaeus vannamei* and *Artemia salina*, activating their enzymatic
1156 antioxidant system (Fernandes et al. 2017; Pretti et al., 2014), however, few data are
1157 available about graphene toxicity in fish. In this study, it was used the fish *Danio rerio*
1158 as biological model, suitable for toxicity studies, including those dealing with
1159 environmental contaminants and NM, as for the fact that exhibit physiological
1160 responses to xenobiotics similar to that occurring in mammals, because the genome is

1161 similar in those animals, having equivalent physiological and immunological responses
1162 (Fako and Furgeson, 2009; Froehlicher et al., 2009; Pyati et al., 2007).

1163 Besides the biochemical responses, organisms also exhibit molecular defenses
1164 that can be activated when a pro-oxidative situation is induced. However, a response at
1165 the molecular level does not always interleaved with a biochemical response, regards
1166 the toxic being evaluated. The nuclear transcription factor NF-E2-related, factor 2
1167 (*nrf2*), plays an important role in this system, activating the expression of several
1168 antioxidant genes, among them are phase II detoxifying enzymes, as GST, also GSH
1169 peroxidase (GPx) enzyme and glutamate cysteine ligase catalytic subunit (*gclc*) gene,
1170 the limiting enzyme for GSH production, thus being directly involved in GSH
1171 concentration (Enomoto et al., 2001; Lewis et al., 2010; Kobayashi and Yamamoto,
1172 2005). Therefore it was the genes chosen for the present study, where a possible
1173 response in *nrf2* gene expression could also lead to a response on *gclc* expression, as
1174 shown in studies by Mishra et al. (2014) and Kowluru and Mishra (2016).

1175 Graphene ability to induce genes of the antioxidant system has already been
1176 showed (Chatterjee et al., 2014). However studies considering the expression of the *nrf2*
1177 gene being affected by nanomaterials are scarce until the present moment, but it is
1178 known that it can be modulated through the exposure of silver nanoparticles in human
1179 renal epithelial cells, directly influencing the GCL-GSH balance inside the cells and its
1180 consequent signaling (Kang et al., 2012). In this study, however, it was not possible to
1181 observe any effect on the expression of the *nrf2* gene in gills, intestine and muscle
1182 (**Figures 3a, 3b, 3c** respectively), where the exposure of the two concentrations of
1183 graphene did not alter the expression in relation to SDS-control group.

1184 The study conducted by Usenko et al. (2008) in zebrafish, had shown that after
1185 48 h of fullerene C₆₀ exposure, the *gclc* gene had up-regulated. Similar data was
1186 observed in the study of Da Rocha et al. (2013) where *i.p.* exposure to fullerol showed
1187 an up-regulation of this gene after 48 h; however, the same was not observed when the
1188 exposure was to single-walled carbon nanotubes (SWCNT). This last result corroborates
1189 with our study, where *gclc* gene expression results had not shown statistical difference
1190 after graphene exposure in gills, intestine and muscle (**Figures 2a, 2b, 2c**, respectively)
1191 as also for the *nrf2* gene. The fact that SWCNT and graphene are similar carbon NM
1192 that differ in morphology, may explain why they exhibit similar effects despite tissue
1193 differences, while fullerol, despite being also a carbon nanomaterial, has functionality
1194 and structure (OH groups) that differ from graphene, perhaps because of this different
1195 effects had been observed in both studies (Jortner e Rao, 2002; Zhang et al., 2010).

1196 The molecular results on this study had not shown statistical difference, and one
1197 possibility that could explain these results it is regards about exposure time. GR
1198 probably did not interfere in the expression of *gclc* and *nrf2* genes due to the short
1199 period (48 h) of exposure; which was insufficient to activate the complex machinery of
1200 antioxidant gene expression system. This hypothesis is supported by the molecular
1201 study from Wu et al. (2014), that had shown the toxic effect of graphene oxide (GO) on
1202 mRNA specific genes in *Caenorhabditis elegans*, showing that GO is able to reduce the
1203 expression of several genes and thus influencing in several pathways, including growth,
1204 describing a direct relation with mortality of the animal; this study however only had
1205 results after a long period of exposure, of about 24 days. Besides, the time statement is
1206 also corroborated by the fact that it was observed a response from the biochemical
1207 antioxidant defense system that would be the first response to a toxin due to its rapid
1208 activation (Storey, 2005).

1209 Reduced glutathione (GSH) is the main cellular thiol antioxidant that acts as
1210 scavenger of reactive oxygen species (ROS) directly or indirectly in cells, and as co-
1211 substrate for many antioxidant phase II enzymes (Halliwell and Gutteridge, 2007;
1212 Harvey et al., 2009). It was observed that exposure to 5 mg/L of graphene caused a
1213 decrease in GSH concentration in gills (**Figure 4a**) and an increase in intestine (**Figure**
1214 **4b**) when compared to SDS-control group. These results, indicates that in gills GR
1215 exposure lead to higher susceptibility to oxidative stress, with less molecules to cope
1216 against the redox alterations, and a similar result also was observed by Chatterjee et al.
1217 (2014) on HepG2 human cells and Liu et al. (2011) on bacterial cells. In the intestine,
1218 GSH levels were induced for maintenance of the redox balance against the toxicant
1219 exposure. Differently, in muscle was not observed alterations on GSH concentration
1220 after the exposure (**Figure 4c**). The same was not observed on brain thought. This organ
1221 showed that reduced glutathione levels can be altered after GR exposure on low and
1222 high concentrations (**Figure 4d**), exhibiting increase when compared to SDS-control,
1223 probably due to increased production of intracellular ROS caused by GR exposure, as
1224 was shown in Fernandes et al. (2017) and Wu et al. (2016).

1225 The activation of enzymes responsible for GSH synthesis is one form to analyze
1226 a response to oxidative stress; the synthesis of GSH is catalyzed by two enzymes, where
1227 GCL is the pacemaker enzyme, and their activity is regulated by the GSH levels that are
1228 present on tissues (White et al., 2003). In this study it was observed that GR exposure
1229 does not seem to had any effect on the enzyme activity in gills (**Figure 5a**) and muscle
1230 (**Figure 5c**), although intestine (**Figure 5b**) and brain (**Figure 5d**) results shown an
1231 increase in GCL activity after GR exposure, on both low and high concentrations. Britto
1232 et al. (2012) showed the reduction in the activity of GCL after fullerene and fullerol
1233 exposure on gills of fish *Cyprinus carpio*. Also in gills of shrimp *L. vannamei* the

1234 exposure to GR showed a reduction in GCL activity (Fernandes et al., 2017). Analyzing
1235 the GSH and GCL results in the intestine, at low concentration of graphene, and brain
1236 on both concentrations, they showed a regulatory mechanism, in with GR seemed to
1237 promote an oxidant environment inside cells causing the induction of the enzyme and,
1238 thus, increasing GSH levels (Halliwell and Gutteridge, 2007).

1239 The GST enzyme is a superfamily of phase II enzymes responsible for cellular
1240 detoxification, which uses GSH as conjugant agent for the reaction process, being
1241 involved on oxidative stress responses and detoxification of several environmental
1242 toxicants (Kim et al., 2010). The modulation of GST activity in different biological
1243 models exposed to different toxicants has already been evaluated on several studies
1244 presented in scientific literature (Da Rocha et al., 2013; Ferreira et al., 2012; Pichardo et
1245 al., 2017; Weber et al., 2014), however, in exposures to CNM was evidenced the
1246 inability to modulate the enzyme. The increased levels of GST found on intestine
1247 (**Figure 6b**) and brain (**Figure 6d**), goes in encounter of the ones observed for GSH and
1248 GCL on these organs, showing the activation of the antioxidant system in front of the
1249 exposure to the low concentration of GR, where the need for more GSH molecules is
1250 being necessary for the GST enzyme to perform the detoxification process that is being
1251 caused by graphene. Similar results were observed on Marchi et al. (2017) where the
1252 exposure to multi-walled carbon nanotubes (MWCNT) in low concentrations of 0.01
1253 and 1.00 mg/L induced the enzyme activity on two polychaete species (*Diopatra*
1254 *neapolitana* and *Hediste diversicolor*) and on Mesaric et al. (2015), that evaluated the
1255 enzyme activity after 48 h exposure to carbon black on *Artemia saline* larvae, showing
1256 an increase of activity at 0.01 and 1.00 mg/L concentrations. The lack of induction
1257 observed on gills (**Figure 6a**) plus the reduction of GSH levels observed indicates that
1258 GR detoxification probably does not happen via phase II enzymes such as the GST

1259 family, as was shown on Ferreira et al. (2012) after fullerol exposure on gills of *C.*
1260 *carpio*; and that GSH antioxidant molecule could be acting alone against the GR toxics
1261 effects on this tissue.

1262 This scenario on gills of *D. rerio*, probably allowed the accumulation of toxic
1263 compounds and leaving this organ more vulnerable to pro-oxidant conditions, expressed
1264 by lipid peroxidation damage. Graphene at the concentration of 50 mg/L seems to be
1265 toxic for gills as can be evidenced by the increase of peroxidized lipids (**Figure 7a**). NM
1266 had already been shown to be toxic to aquatic organisms, especially in gills of *C. carpio*
1267 exposed to fullerene (Britto et al., 2012, Ferreira et al., 2012) and in polychaete *D.*
1268 *neapolitana* and *H. diversicolor* exposed to nanotubes, generating an increase in the
1269 levels of peroxidized lipids in these animals (Mesaric et al., 2015). The similar result also
1270 was observed in gills of shrimp *L. vannamei* after graphene exposure (Fernandes et al.,
1271 2017). However, *D. rerio* antioxidant defense system in the intestine showed to be
1272 efficient against oxidative stress (**Figure 7b**), showing a better capacity for redox
1273 regulation than in human intestinal cell line Caco-2, where lipid damage was observed
1274 after the exposure to SWCNT (Pichardo et al., 2012). The brain of *D. rerio* appears to
1275 efficiently protect itself against CNM, where lipid damage was not exhibited after *i.p.*
1276 exposure to graphene (**Figure 7d**), as well other study showed that, SWCNT-PEG *i.p.*
1277 exposure did not induced oxidative damage (Weber et al., 2014).

1278 Morphological, pathological, structural and cellular changes can lead to organ
1279 dysfunction and compromise the animal life, especially in gills, a multifunctional and
1280 complex organ that make intimate contact with the surrounding water, being responsible
1281 for osmoregulation and respiration process in fish from freshwater. In fact, histological
1282 changes were observed after 5 mg/L and 50 mg/L graphene exposure on gills, causing
1283 moderate and severe pathological hyperplasia, respectively (**Figure 8a**), while in the

1284 intestine was not observed differences between groups (**Figure 8b**). Similar results were
1285 found on *D. rerio* exposed to MWCNT (Filho et al., 2014), being observed hyperemia,
1286 aneurism and inflammatory focus on gills, and no alterations at intestine cells, although
1287 MWCNT particles could be observed on the intestine lumen. These observations
1288 indicate how sensible gills are to the presence of CNM, and that intestine has a
1289 protection against these materials, by the presence of muscle layers that prevent the
1290 contact of the nanomaterial with intestine cells when exposed through *i.p.*, or by the
1291 mucus secreted by the epithelial cells that act as a barrier against the penetration of
1292 these materials when exposed through feed or water (Cone, 2009).

1293 GR has already being shown to cause morphological changes on kidney of rats
1294 exposed on low and high concentrations (Patlolla et al., 2016). In this study, muscle
1295 suffered pathological damage, being observed edema and inflammatory infiltrates
1296 between the muscular fibers after exposure to both concentrations of graphene (**Figure**
1297 **8c**), that could be caused by the presence and accumulation of NM in these regions after
1298 *i.p.* injections. Besides, it was observed in brain that exposure to both GR
1299 concentrations caused inflammatory responses, with ganglionic proliferations,
1300 increased microglia cells and moderate edema in G1, and increased ganglionic
1301 proliferation leading to a larger number of astrocytes, and severe edema in G2 (**Figure**
1302 **8d**). These results are supported by Weber et al., (2014), that found similar responses on
1303 *D. rerio* brains after SWCNT-PEG exposure.

1304 **6. Conclusions**

1305 The results found in this study showed that graphene at short-time exposure
1306 induced deleterious effects in gills, muscle and brain considering histological damages.
1307 Besides, the modulation of the antioxidant system was observed in some organs, like,
1308 intestine. These results showed that direct exposure to GR modulated the antioxidant

1309 system of zebrafish in different tissues, causing lipid damage in some and
1310 morphological alterations in others. However, the activation of key genes of the
1311 antioxidant system was not observed in a 48 h exposure, for that, a longer exposure
1312 period are suggested to evaluate these effects. Although each tissue showed different
1313 responses to GR exposure it is possible to observe, when analyzing all the results, that
1314 this NM could lead to tissue damage, compromising its function and endangering the
1315 animal welfare. Because GR use is increasingly, a detailed study on the pathway of
1316 activation of this NM in short and especially long exposure periods becomes necessary
1317 to know the systemic effect that GR exerts on the animal.

1318 **Acknowledgments:** The authors would like to thank CNPq for financial support
1319 (Universal program, process number 476770/2013-0). Amanda Lucena Fernandes is a
1320 graduate fellow at Coordenação de Aperfeiçoamento de Pessoal de Nível Superior
1321 (CAPES). José M. Monserrat, Clascídia Furtado, Adelina Pinheiro Santos are research
1322 fellows at CNPq. Clascídia Furtado, Adelina Santos, Juliane Ventura-Lima and José M.
1323 Monserrat are members of the nanotoxicology network (MCTI/CNPq, Proc.
1324 552131/2011-3). Conflicts of interest: none.

1325 **References**

- 1326 Aitken, R.J., Chaudhry, M.Q., Boxall, A.B.A., Hull, M. 2006. Manufacture and
1327 use of nanomaterials: Current status in the UK and global trends. *Occupat. Med-Oxford*.
1328 56, 300–306.
- 1329 Chatterjee, N., Eom, H.J., Cho, J. 2014. A systems toxicology approach to the
1330 surface functionality control of graphene-cell interactions. *Biomaterials*. 35, 1109-1127.
- 1331 Chen, D., Tang, L.H. Li, J. 2010. Graphene-based materials in electrochemistry.
1332 *Chem. Soc. Rev.* 39, 3157 -3180.
- 1333 Cone, R.A. 2009. Barrier properties of mucus. *Adv. Drug Deliv. Rev.* 61, 75–85.
- 1334 Da Rocha, A.M., Salomão de Freitas, D.P., Burns, M., Vieira, J.P., de la Torre,
1335 F.R., J.M. Monserrat, J.M. 2009. Seasonal and organ variations in antioxidant capacity,
1336 detoxifying competence and oxidative damage in freshwater and estuarine fishes from
1337 Southern Brazil. *Comp. Biochem. Physiol. C*. 150, 512–520.
- 1338 Da Rocha, A.M., Ferreira, J.R., Barros, D.M., Pereira, T.C.B., Bogo, M.R.,
1339 Oliveira, S., Geraldo, V., Lacerda, R.G., Ferlauto, S., Ladeira, L.O., Veloso, M.,
1340 Pinheiro, V.B., Monserrat, J.M. 2013. Gene expression and biochemical responses in
1341 brain of zebrafish *Danio rerio* exposed to organic nanomaterials: Carbon nanotubes
1342 (SWCNT) and fulleranol (C₆₀ (OH)_{18–22}(OK₄)). *Comp. Biochem. Physiol. A*. 165, 460–
1343 46.
- 1344 Enomoto, A., Itoh, K., Nagayoshi, E., Haruta, J., Kimura, T., O'Connor, T.,
1345 Harada, T., Yamamoto, M. 2001. High sensitivity of Nrf2 knockout mice to
1346 acetaminophen hepatotoxicity associated with decreased expression of ARE-regulated
1347 drug metabolizing enzymes and antioxidant genes. *Toxicol. Sci.* 59, 169-77.
- 1348 Fako, V.E., Furgeson, D.Y. 2009. Zebrafish as a correlative and predictive
1349 model for assessing biomaterial nanotoxicity. *Adv. Drug Deliv. Rev.* 61, 478–486.
- 1350 Fernandes, A.L., Josende, M.E., Nascimento, J.P., Santos, A.P., Sahoo, S.K.,
1351 Silva Júnior, F.M.R., Romano, L.A., Furtado, C.A., Wasielesky, W., Monserrat, J.M.,

- 1352 Ventura-Lima, J. 2017. Exposure to graphene through diet induces oxidative stress
1353 situation and histological changes in the marine shrimp *Litopenaeus vannamei*. Toxicol.
1354 Res. In press. DOI: 10.1039/c6tx00380j
- 1355 Ferreira, J.L.R., Barros, D.M., Geracitano, L.A., Fillmann, G., Fossa, C.E.,
1356 Almeida, E.A., Prado, M.C., Neves, B.R.A., Pinheiro, M.V.B., Monserrat, J.M. In vitro
1357 exposure to fullerene C₆₀ influences redox state and lipid peroxidation in brain and gills
1358 from *Cyprinus carpio* (Cyprinidae). Environ. Toxicol. and Chem. 31, 5, 961–967.
- 1359 Filho, J.S., Matsubara, E.Y., Franchi, L.P., Martins, I.P., Rivera, L.M.R.,
1360 Rosolen, J.M., Grisolia, C.K. 2014. Evaluation of carbon nanotubes network toxicity in
1361 zebrafish (*Danio rerio*) model. Environ. Res. 134, 9–16.
- 1362 Fischer, H.C., Chan, W. 2007. Nanotoxicology: the growing need for *in vivo*
1363 study. Curr. Opin. Biotechnol. 18, 565–571.
- 1364 Froehlicher M., Liedtke, A., Groh, K.J., Neuhauss, S.C., Segner, H., Eggen, R.I.
1365 2009. Zebrafish (*Danio rerio*) neuromast: promising biological endpoint linking
1366 developmental and toxicological studies. Aquat. Toxicol. 95, 307–19.
- 1367 Habig, W.H., Pabst, M.J., Jakoby, W.B. 1974. Glutathione-S-transferases: The
1368 first enzymatic step in mercapturic acid formation. Biol. Che. 249, 7130-7139.
- 1369 Harvey, C.J., Thimmulappa, R.K., Singh, A., Blake, D.J., Ling, G.,
1370 Wakabayashi, N., Fujii, J., Myers, A., Biswal, S. 2009. Nrf2-regulated glutathione
1371 recycling independent of biosynthesis is critical for cell survival during oxidative stress.
1372 Free Rad. Biol. Med. 15, 46(4), 443-53.
- 1373 Huang, C., Li, C., Shi G. 2012. Graphene based catalysts. Energy Environ. Sci.
1374 5, 8848-8868.
- 1375 Jaworski, S., Sawosz, E., Grodzik, M., Winnicka, A., Prasek, M., Wierzbicki,
1376 M., Chwalibog, A. 2013. In vitro evaluation of the effects of graphene platelets on
1377 glioblastoma multiform cells. Int. J. Nanomedicine. 8, 413-420.

- 1378 Kang, S.J., Lee, Y.J., Lee, E.K., Kwak, M.K. 2012. Silver nanoparticles-
1379 mediated G2/M cycle arrest of renal epithelial cells is associated with NRF2-GSH
1380 signaling. *Toxicol. Lett.* 211, 334–341.
- 1381 Khan, U., Porwal, H., O'Neill, A., Nawaz, K., May, P., Coleman, J. N. 2011.
1382 Solvent-Exfoliated Graphene at Extremely High Concentration. *Langmuir.* 17, 9077–
1383 9082.
- 1384 Kim, I.H., Dahms, H.V., Rhee, J.S., Lee, Y.M., Lee, J., Han, K.N., Lee, J.S.
1385 2010. Expression profile of seven glutathione-S-transferase (GST) genes in cadmium-
1386 exposed river pufferfish (*Takifugu obscurus*). *Comp. Biochem. Physiol. C.* 151: 99-106.
- 1387 Kobayashi, M., Yamamoto, M. 2005. Molecular mechanisms activating the Nrf2-
1388 Keap1 pathway of antioxidant gene regulation. *Antiox. Redox Signal.* 7 (3-4), 385-394.
- 1389 Kowluru, R.A., and Mishra, M. Epigenetic regulation of redox signaling in
1390 diabetic retinopathy: Role of Nrf2. *Free Rad. Biol. Med.*
1391 <http://dx.doi.org/10.1016/j.freeradbiomed.2016.12.030>. In press.
- 1392 Lawrence, C., 2007. The husbandry of zebrafish (*Danio rerio*): A review.
1393 *Aquaculture*, 269, 1–20.
- 1394 Lewis, K.N, Mele, J., Hayes, J.D., Buffenstein, R. 2010. Nrf2, a guardian of
1395 health span and gatekeeper of species longevity. *Integr. Comp. Biol.* 50, 829-43.
- 1396 Li, Y., Liu, Y., Fu, Y., Wei, T., Le Guyader, L., Gao, G., Liu, R.S., Chang, Y.Z.,
1397 Chen, C. 2012. The triggering of apoptosis in macrophages by pristine graphene
1398 through the MAPK and TGF-beta signaling pathways. *Biomaterials.* 33, 402-411.
- 1399 Mafra, D.L., 2008. Dispersão de fônons na vizinhança do ponto de Dirac do
1400 grafeno por espalhamento Raman, Belo Horizonte, Universidade Federal de Minas
1401 Gerais.
- 1402 Marchi, L., Neto, V., Pretti, C., Figueira, E., Chiellini, F., Soares, A.M.V.M.,
1403 Freitas, R. 2017. Physiological and biochemical responses of two keystone polychaete
1404 species: *Diopatra neapolitana* and *Hediste diversicolor* to multi-walled carbon
1405 nanotubes. *Environ. Res.* 154, 126–138.

- 1406 Markovic, Z.M., Trajkovic, H.L., Markovic, T.M.B., Kepi, P.D., Arsikin, M.K.,
1407 Jovanovi, P.S., Pantovic, A.C., Dramićanin, M.D., Trajkovic, V.S. 2011. *In vitro*
1408 comparison of the photothermal anticancer activity of graphene nanoparticles and
1409 carbon nanotubes. *Biomaterials*. 32, 1121- 1129.
- 1410 Matés J.M, Pérez-Gómez C, Castro I, N., 1999. Antioxidant enzymes and human
1411 diseases. *Clin. Biochem*. 32, 595–603.
- 1412 Mishra, M., Zhong, Q., Kowluru, R.A. 2014. Epigenetic modifications of Nrf2-
1413 mediated glutamate–cysteine ligase: Implications for the development of diabetic
1414 retinopathy and the metabolic memory phenomenon associated with its continued
1415 progression. *Free Rad. Biol. Med*. 75, 129–139.
- 1416 Nguyen, P, Berry, V. 2012. Graphene interfaced with biological cells:
1417 Opportunities and challenges. *The J. Phys. Chem. Lett*. 3, 1024–1029
- 1418 Oakes, K.D., Kraak, G.J.V. 2003. Utility of the TBARS assay in detecting
1419 oxidative stress in white sucker (*Catostomus commersoni*) populations exposed to pulp
1420 mill effluent. *Aquat. Toxicol*. 63, 447-460.
- 1421 Oberdörster, E. 2004. Manufactured nanomaterials (fullerenes, C₆₀) induce
1422 oxidative stress in the brain of juvenile largemouth bass. *Envir. Hea. Perspec*. 112,
1423 1058-1062.
- 1424 Park, S.; Mohanty, N., Suk, J.W., Nagaraja, A., An, J.H., Piner, R.D., Cai,
1425 W.W., Dreyer, D.R., Berry, V., Ruoff, R.S. 2011. Biocompatible, robust free-standing
1426 paper composed of a TWEEN/graphene composite. *Adv. Mater*. 22, 1736–1740.
- 1427 Patlolla, A.K., Randolph, J., Kumari, S.A., Tchounwou, P.B. 2016. Toxicity
1428 evaluation of graphene oxide in kidneys of Sprague-Dawley rats. *Int. J. Environ. Res.*
1429 *Public Health*. 13, 380.
- 1430 Pichardo, S., Gutiérrez-Praena D., Puerto, M., Sánchez, E., Grilo, A., Cameán,
1431 A.M., Jos, A. 2012. Oxidative stress responses to carboxylic acid functionalized single
1432 wall carbon nanotubes on the human intestinal cell line Caco-2. *Toxicol. in Vitro*. 26,
1433 672–677.

- 1434 Pretti, C., Oliva, M., Pietro, R.D., Monni, G., Cevasco, G., Chiellini, F., Pomelli,
1435 C., Chiappe, C. 2014. Ecotoxicity of pristine graphene to marine organisms. *Ecotoxicol.*
1436 *Environ. Saf.* 10, 138–145.
- 1437 Pyati, U.J., Looka, A.T., Hammerschmidt, M. 2007. Zebrafish as a powerful
1438 vertebrate model system for in vivo studies of cell death. *Semin. Cancer Biol.* 17, 154–
1439 165.
- 1440 Rosa, C.E., Kuradomi, R.Y., Almeida, D.V., Lannes, C.F.C., Figueiredo, M.A.,
1441 Dytz, A.G. 2010. GH overexpression modifies muscle expression of antioxidant
1442 enzymes and increases spinal curvature of old zebrafish. *Exp. Gerontol.* 45, 459–466.
- 1443 Stankovich S, Dikin, D.A., Dommett, G.H., Kohlhaas, K.M., Zimney, E.J., Stach,
1444 E.A., Piner, R.D., Nguyen, S.B.T, Ruoff, R.S. 2006. Graphene-based composite
1445 materials. *Nature.* 442, 282-286.
- 1446 Storey, K.B. 2005. *Functional Metabolism: Regulation and Adaptation.* Ed. John
1447 Wiley & Sons. Hoboken, NJ.
- 1448 Zar, J.H. 1984. *Biostatistical analysis.* Ed. Prentice Hall. NJ.
- 1449 Zhang, Y., Ali, S.F., Dervishi, E., Xu, Y., Li, Z., Casciano, D., Biris, A.S. 2010.
1450 Cytotoxicity effects of graphene and single-wall carbon nanotubes in neural
1451 phaeochromocytoma-derived PC12 cells. *ACS Nano.* 4, 3181-3186.
- 1452 Zhang, X., Yin, J., Peng, C., Hu, W., Zhu, Z., Li, W., Fan, C., Huang, Q. 2011.
1453 Distribution and biocompatibility studies of graphene oxide in mice after intravenous
1454 administration. *Carbon.* 49, 986-995.
- 1455 Weber, G.E.B., Bosco, L.D., Gonçalves, C.O.F., Santos, A.P., Fantini, C.,
1456 Furtado, C.A., Parfitt, G.M., Peixoto, C., Romano, L.A., Vaza, B.S., Barros, D.M. 2014.
1457 Biodistribution and toxicological study of PEGylated single-wall carbon nanotubes in
1458 the zebrafish (*Danio rerio*) nervous system. *Toxicol. Appl. Pharmacol.* 280, 3, 484-92.
- 1459 White, C.C, Viernes, H., Krejsa, C.M., Botta, D., Kavanagh, T.J. 2003.
1460 Fluorescence-based microtiter plate assay for glutamate-cysteine ligase activity. *Anal.*
1461 *Biochem.* 318, 175-180.

1462 Wu, Q., Zhao, Y., Zhao, G., MS, Wang, D. 2014. microRNAs control of in vivo
1463 toxicity from graphene oxide in *Caenorhabditis elegans*. *Nanomedicine: NBM.* 10, 7,
1464 1401–1410.

1465 Wu, W., Yan, L., Wu, Q., Li, Y., Li, Q., Chen, S., Yang, Y., Gu, Z., Xu, H., Yin,
1466 Z.Q. 2016. Evaluation of the toxicity of graphene oxide exposure to the eye.
1467 *Nanotoxicology.* 10, 9, 1329-1340.

1468 Yang, K., Gong, H. Shi, X., Wan, J., Zhang, Y., Liu, Z. 2013. In vivo
1469 biodistribution and toxicology of functionalized nano-graphene oxide in mice after oral
1470 and intraperitoneal administration. *Biomaterials* 34, 2787-2795.

1471 Yuan, J., Gao, H., Ching, C.B. 2011. Comparative protein profile of human
1472 hepatoma HepG2 cells treated with graphene and single-walled carbon nanotubes: an
1473 iTRAQ-coupled 2D LCMS/MS proteome analysis. *Toxicol. Lett.* 207, 213-221.
1474

1475 7. Appendices

1476 **Figure 1.** (a), (b) and (c) Transmission electron microscopy (TEM) images of graphene
1477 nanosheets obtained from diluted dispersion 1800x in NMP.

1478

1479 **Figure 2.** Gene expression of glutamate-cysteine-ligase catalytic subunit (*Gclc*)
1480 in gills (a), intestine (b) and muscle (c) of *D. rerio* treated with MilliQ water (control),
1481 SDS detergent, graphene suspension of 5 mg/L and graphene suspension of 50 mg/L.
1482 Data are expressed as relative gene expression considering the SDS-control group gene
1483 expression as 1. Columns follow by the same letter are not statistically different in
1484 between by the Newman-Keuls test ($p < 0.05$).

1485

1486 **Figure 3.** Gene expression of transcription factor *Nrf2* in in gills (a), intestine (b) and
1487 muscle (c) of *D. rerio* treated with MilliQ water (control), SDS detergent, graphene
1488 suspension of 5 mg/L concentration and graphene suspension of 50 mg/L . Data are
1489 expressed as relative gene expression considering the SDS-control group gene
1490 expression as 1. Columns follow by the same letter are not statistically different in
1491 between by the Newman-Keuls test ($p < 0.05$).

1492

1493 **Figure 4.** Glutathione concentration levels (expressed as nmol of GSH/30min/mg of
1494 protein) in gills (a), intestine (b), muscle (c) and brain (d) of *D. rerio* exposed to
1495 different treatments over 48 h, groups are detailed above. Data are expressed as average
1496 ± 1 standard error (n=4-5). Columns follow by the same letter are not statistically
1497 different in between by the Newman-Keuls test ($p < 0.05$).

1498

1499 **Figure 5.** Levels of glutamate-cysteine-ligase activity (expressed as nmol of
1500 GSH/30min/mg of protein) standardized by glutathione concentration in gills (a),
1501 intestine (b), muscle (c) and brain (d) of *D. rerio* exposed to different treatments over 48
1502 h. Control: fish that were injected with MilliQ water; SDS: fish that were exposed to
1503 SDS detergente; G1: fish that were exposed to graphene solution with concentration of
1504 5 mg/L; G2: fish that were exposed to graphene solution with concentration of 50mg.
1505 Data are expressed as average ± 1 standard error (n=4-5). Columns follow by the same
1506 letter are not statistically different in between by the Newman-Keuls test ($p < 0.05$).

1507

1508 **Figure 6.** Activity of glutathione-S-transferase (expressed as nmol of CDNB
1509 conjugated/min/mg of protein) in gills (a), intestine (b), muscle (c) and brain (d) of *D.*
1510 *rerio* exposed to different treatments over 48 h, groups are detailed above. Data are
1511 expressed as average ± 1 standard error (n=4-5). Columns follow by the same letter are
1512 not statistically different in between by the Newman-Keuls test ($p < 0.05$). CDNB: 1-
1513 chloro-2,4-dinitrobenzene

1514

1515 **Figure 7.** Thiobarbituric reactive substances acid (TBARS) levels (expressed as nmol
1516 od MDA/mg of protein) in gills (a), intestine (b), muscle (c) and brain (d) of *D. rerio*
1517 exposed to different treatments over 48h, groups are detailed above. Data are expressed
1518 as average ± 1 standard error (n=4-5). Columns follow by the same letter are not
1519 statistically different in between by the Newman-Keuls test ($p < 0.05$). MDA:
1520 malondialdehyde.

1521

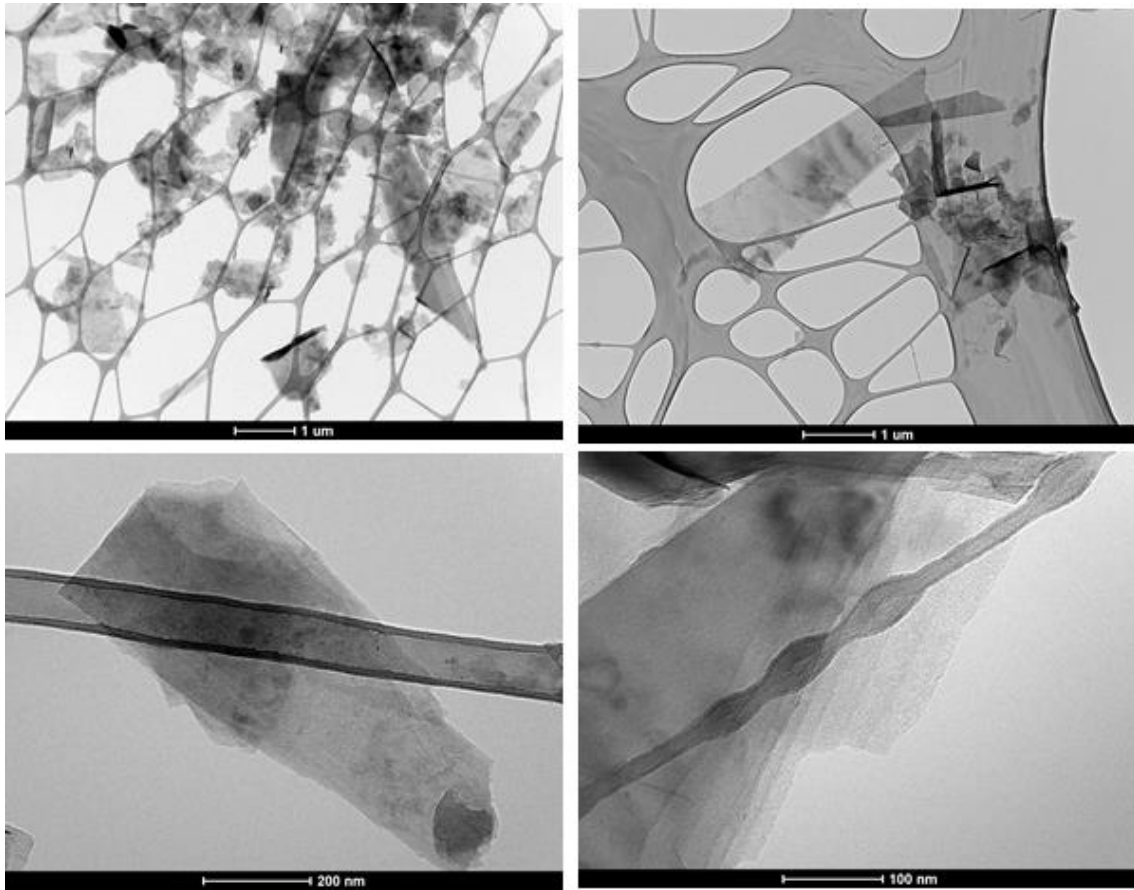
1522 **Figure 8.** Histological analyses of gills (a), intestine (b), muscle (c) and brain (d) of *D.*
1523 *rerio*. Experimental groups are indicated by control (injected with MilliQ), SDS

1524 (injected with SDS detergent), G1 (injected with graphene solution on a concentration
1525 of 5mg) and G2 (injected with a graphene solution on concentration of 50mg), n=6.

1526

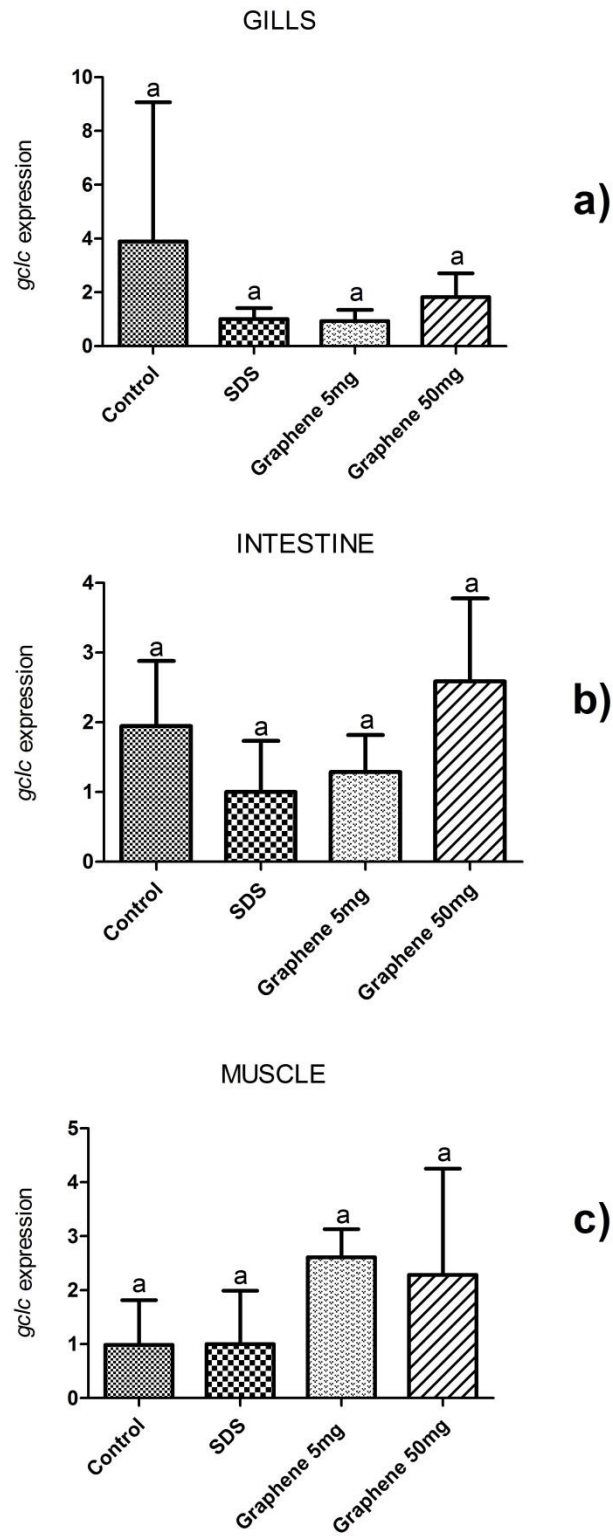
1527 **Table 1.** *Danio rerio* gene-specific primers used for quantitative polymerase chain
1528 reaction expression (RT-Pcr) analysis.

1529

1530 **Figures**

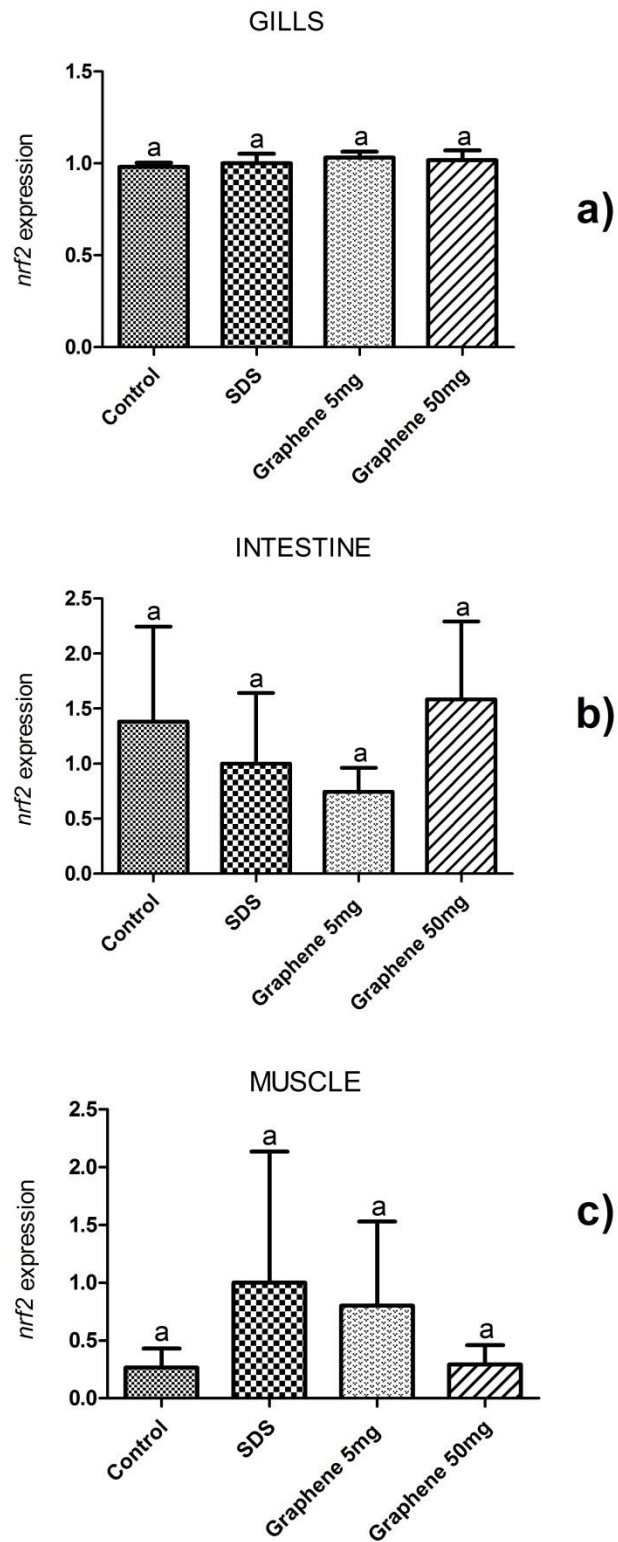
1531

1532 **Figure 1.**



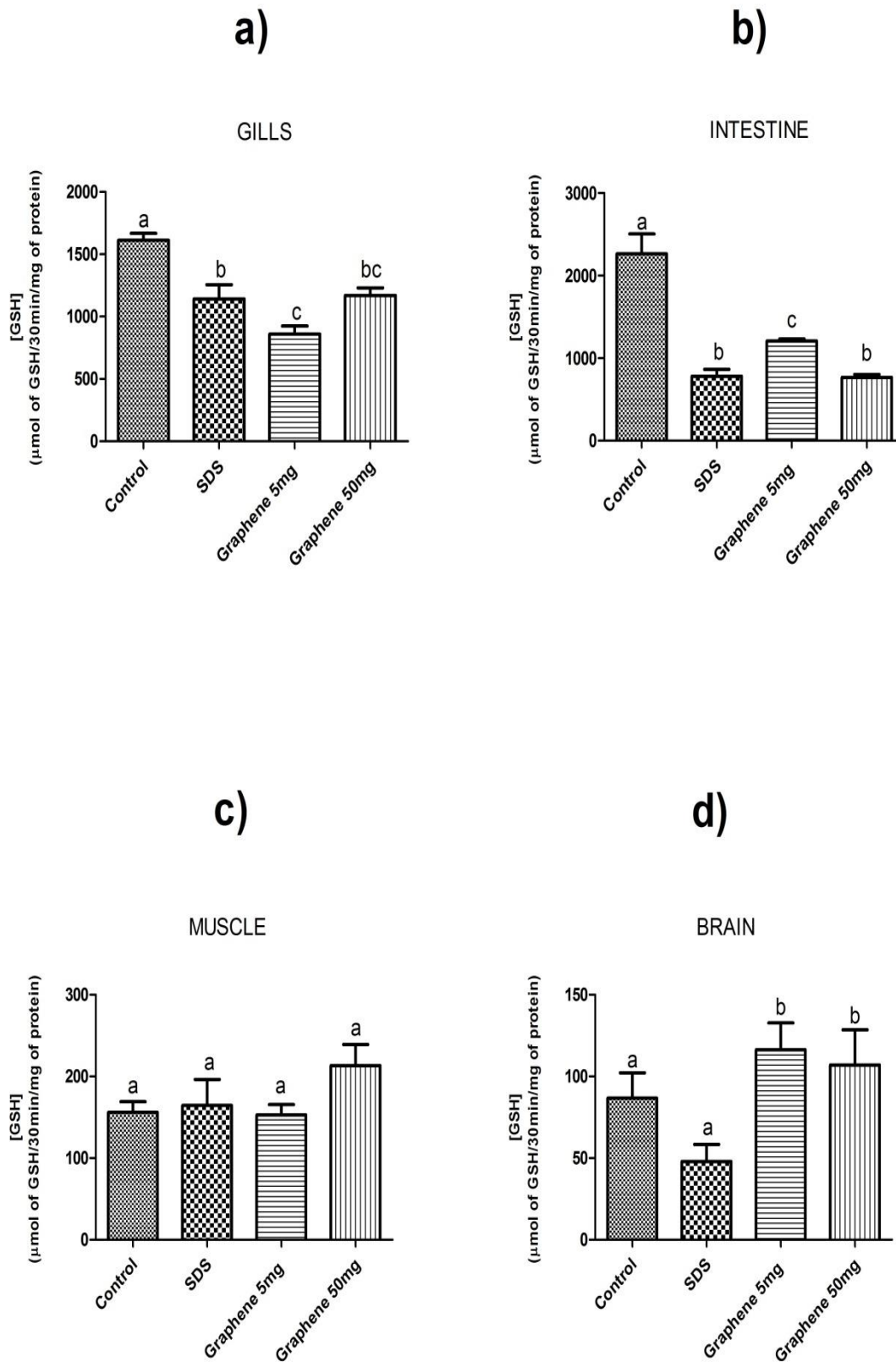
1533

1534 **Figure 2.**



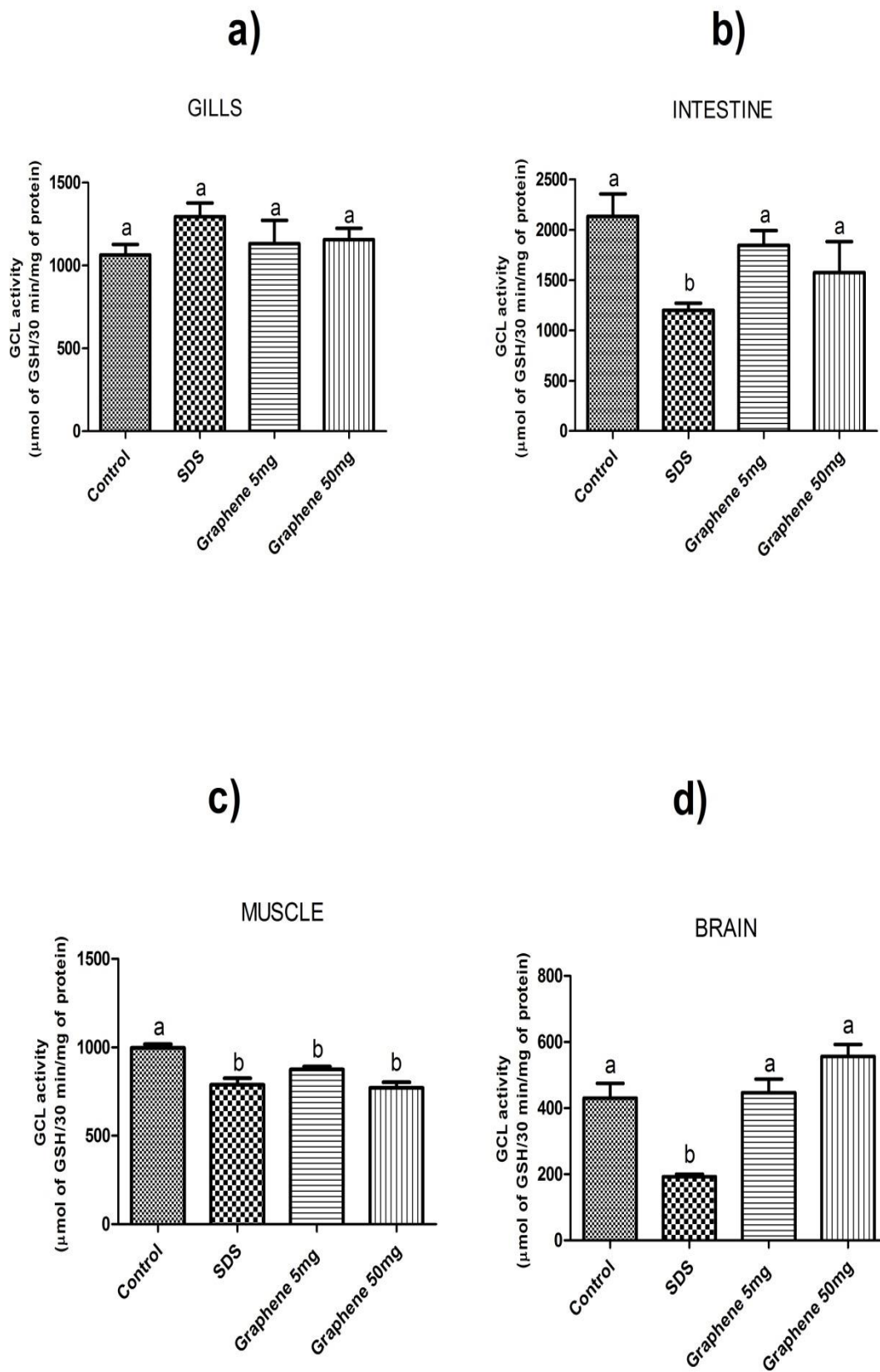
1535

1536 **Figure 3.**



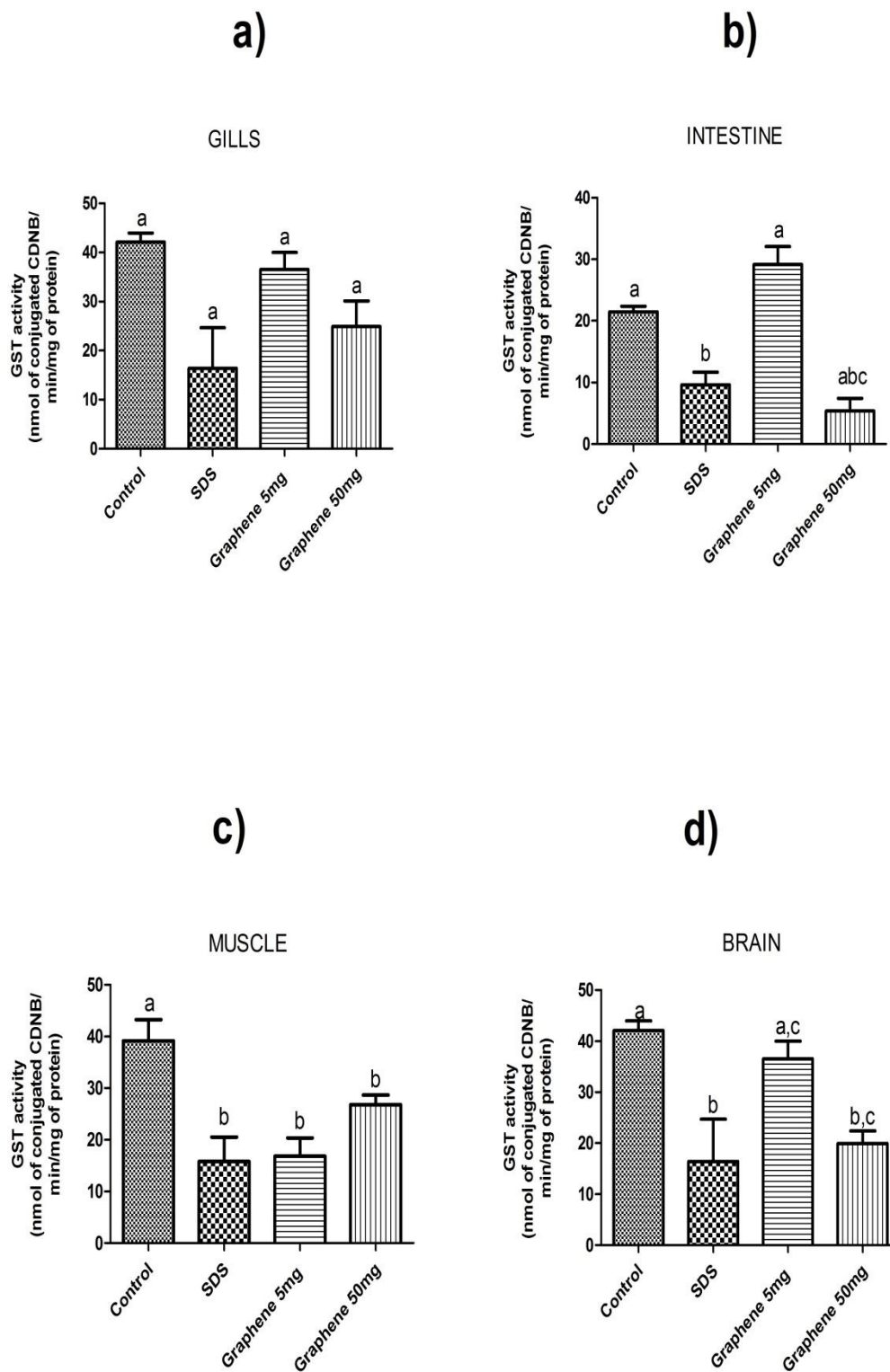
1537

1538 **Figure 4.**



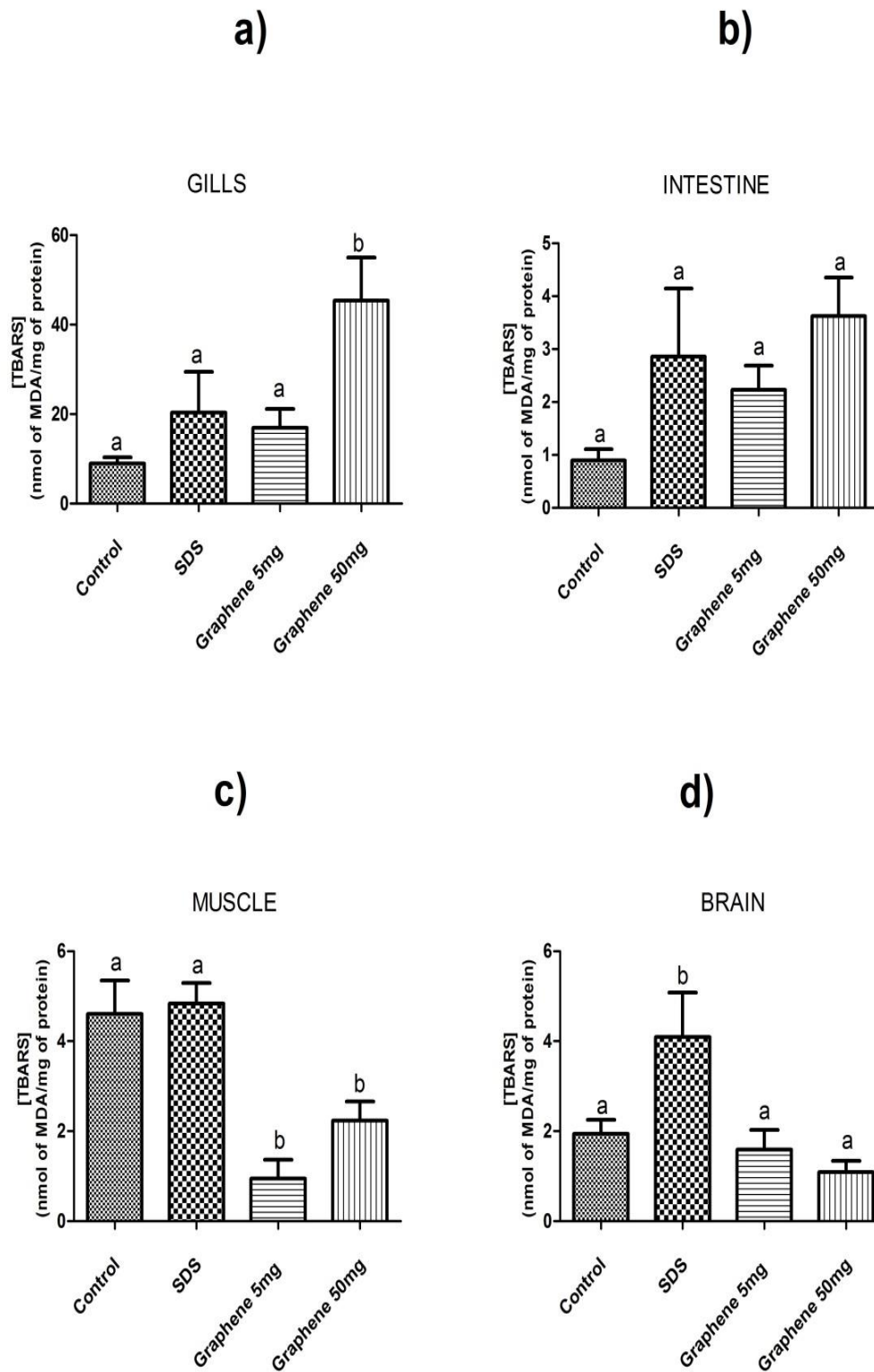
1539

1540 **Figure 5.**



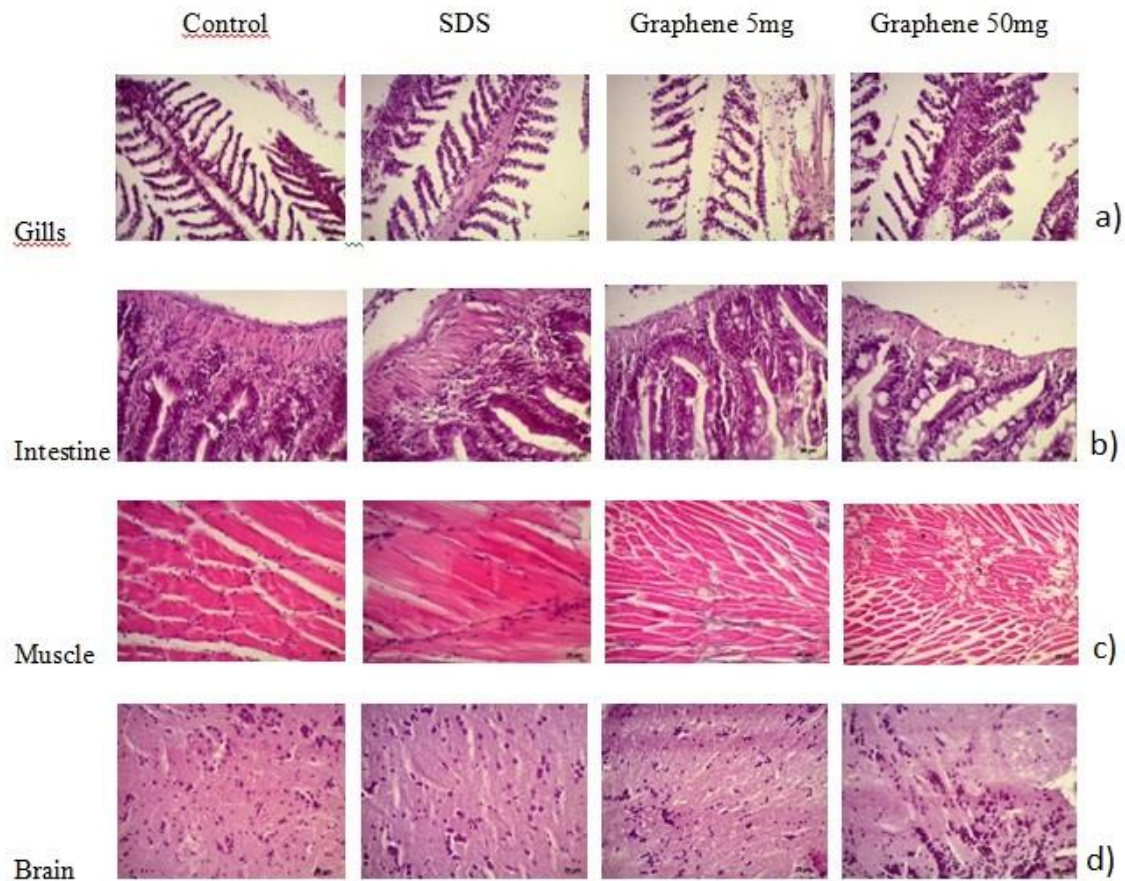
1541

1542 **Figure 6.**



1543

1544 **Figure 7.**



1545
1546 **Figure 8.**

1547

1548

1549

| Gene | Primer sequence | GenBank accession n° |
|------------------|--|----------------------|
| 1553 <i>nrf2</i> | F: 5'-TGTTGGTTCGGAGGCTCTTAA- 3' R: 5'-AGGCCATGTCCACACGTACA- 3' | NM_182889.1 |
| 1555 <i>gclc</i> | F: 5'-AGGGGATTCCCCAGGTTAG- 3' R: 5'-TTTTCAACAGGTGTGGGTTTGT- 3' | NM_199277.2 |
| 1557 <i>ef1a</i> | F: 5'-ACATCAAGAAGATCGGCTACAAC- 3' R: 5'-GACCCACAGGTACAGTTCCAATA- 3' | NM_131263.1 |
| 1559 <i>18S</i> | F: 5'-TGCATGGCCGTTCTTAGTTG- 3' R: 5'-AGTCTCGTTCGTTATCGGAATGA- 3' | NM_001098396 |

1561

1562

1563 **Table 1.**

1564 **7. Discussão Geral**

1565 Nesta dissertação estão inclusos dois trabalhos, no primeiro trabalho o foco se
1566 manteve em avaliar a capacidade do grafeno em induzir um cenário oxidativo em
1567 diferentes tecidos de *Litopenaeus vannamei*. O segundo trabalho, foi centralizado nos
1568 mecanismos de defesa e efeitos que a exposição ao grafeno pode causar aos tecidos de
1569 *Danio rerio*. Foram escolhidas diferentes concentrações, pois no primeiro estudo a
1570 exposição ocorreu juntamente à ração, que foi oferecida 2x por dia durante um mês,
1571 recriando desta forma uma situação ambiental, pois, se sabe que o grafeno não é solúvel
1572 em água porem possui a capacidade de aderir ao substrato; o camarão sendo uma
1573 espécie bentônica estaria em contato direto com o substrato no ambiente e poderia
1574 acabar facilmente ingerindo estes nanomateriais junto à alimentação. Diferentemente,
1575 no segundo estudo já havíamos observado que o grafeno possui a capacidade de induzir
1576 estresse oxidativo, portanto, escolhemos realizar uma exposição intraperitoneal para
1577 assegurar a dose exata a que estávamos expondo o animal. Neste caso, foram escolhidas
1578 diferentes concentrações, baixa e alta (5 e 50 mg/L, respectivamente), para testar se
1579 produziriam efeitos tóxicos diferentes considerando o comportamento de agregação de
1580 partículas quando o grafeno está em grande quantidade, e quais mecanismos de defesa
1581 seriam ativados frente à exposição.

1582 No 1º trabalho, o efeito da exposição ao grafeno ficou caracterizado pela
1583 modulação do sistema antioxidante enzimático do animal, com aumento da produção de
1584 ROS e na síntese de glutathiona reduzida, tanto nas brânquias quanto no hepatopâncreas.
1585 Também foi observada uma diminuição na atividade da enzima GCL em brânquias e
1586 aumento no hepatopâncreas, enquanto que a atividade da GST diminuiu no
1587 hepatopâncreas e aumentou em brânquias. Estes resultados mostram que o dano no
1588 hepatopâncreas foi significativo, onde uma grande concentração de GSH foi necessária

1589 para agir contra a alta quantidade de ROS neste tecido. Porém, com a redução da
1590 atividade da GST as chances do crustáceo se detoxificar ficaram diminuídas; enquanto
1591 que nas brânquias a regulação ocorreu de modo que aumentasse a atividade da GST,
1592 desta forma não se tornando necessária tantas moléculas de GSH e por isso a atividade
1593 baixa de GCL, indicando que a brânquia possui melhor capacidade de detoxificação que
1594 o hepatopâncreas considerando a atividade da GST.

1595 Além disso, a capacidade antioxidante total aumentou, em brânquias e
1596 hepatopâncreas, provavelmente devido a grande concentração de GSH, entretanto o
1597 dano lipídico não foi evitado nestes tecidos, onde um aumento nos níveis de TBARS
1598 (substâncias reativas ao tiobarbitúrico) foi evidenciado. Também foi observado o efeito
1599 do grafeno em induzir genotoxicidade nestes tecidos, gerando dano de DNA em
1600 brânquias e hepatopâncreas. Por fim, foi possível observar alterações histopatológicas
1601 nas células do hepatopâncreas, sendo este o tecido mais lesionado com a exposição.
1602 Vale lembrar que o hepatopâncreas é o órgão responsável pela metabolização de todos
1603 os compostos que o animal entra em contato, então danos nesse tecido comprometem a
1604 capacidade de sobrevivência do animal. Nenhum resultado foi observado em músculo
1605 do camarão após a exposição. Os resultados obtidos com esse estudo corroboram com
1606 os que estão presentes na literatura atual, mostrando a capacidade do grafeno em induzir
1607 estresse oxidativo em células de mamíferos, células bacterianas e outras espécies de
1608 crustáceo, como *Artemia salina*.

1609 No 2º trabalho a exposição ao grafeno não foi capaz de modular o sistema
1610 antioxidante do animal em nível molecular, e os genes marcadores de estresse oxidativo
1611 *nrf2* e *gclc* não sofreram alteração em sua expressão. Entretanto, o sistema enzimático
1612 foi ativado, após a exposição a 5 mg/L a concentração de GSH em brânquias diminuiu,
1613 aumentou no intestino e no cérebro, que também aumentou após a exposição a 50mg/L.

1614 A atividade da GCL aumentou após a exposição às duas concentrações no intestino e
1615 cérebro, enquanto que a atividade da GST aumentou somente após a exposição de
1616 5mg/L nestes mesmos tecidos. Em outros estudos, a ativação destas enzimas já tinha
1617 sido testada frente à exposição de outros nanomateriais, entretanto, este estudo é o
1618 primeiro a mostrar alterações na atividade destas enzimas. A falta de ativação da GST e
1619 pouca concentração de GSH em brânquias associado à exposição gerou um aumento no
1620 nível de peroxidação lipídica após a exposição à menor concentração. Estudos com
1621 outros nanomateriais de carbono também mostram induzir dano oxidativo em brânquias
1622 de peixes, como *D. rerio* e *C. carpio*, evidenciando-se a fragilidade das brânquias frente
1623 a esse nanomateriais. Alterações morfológicas também foram observadas em brânquias,
1624 cérebro e músculo com histopatologias de grau moderado a severo, resultados que
1625 corroboram com os disponíveis na literatura referente a diferentes tipos de grafeno e
1626 outros nanomateriais de carbono.

1627 Apesar nas diferenças em exposição dos dois trabalhos, a capacidade do grafeno
1628 em ativar defesas antioxidantes e provocar alterações histopatológicas em tecidos de
1629 espécies aquáticas se comprovou em ambos, entretanto, o curto tempo de exposição do
1630 2º trabalho pareceu ser o limitante para observar efeitos de biomarcadores moleculares
1631 de estresse oxidativo.

1632 **8. Bibliografia Geral**

- 1633 Aitken, R.J., Chaudhry, M.Q., Boxall, A.B.A., Hull, M., 2006. Manufacture and
1634 use of nanomaterials: Current status in the UK and global trends. *Occupat. Med-*
1635 *Oxford.*, 56, 300–306.
- 1636 Bachere, E., 2000. Shrimp immunity and disease control. *Aquaculture.*, 191, 3–
1637 11.
- 1638 Chen, D., Tang, L.H. Li, J., 2010. Graphene-based materials in electrochemistry.
1639 *Chem. Soc. Rev.*, 39, 3157 -3180.
- 1640 Chen, M., Yin, J., Liang, Y., Yuan, S., Wang, F., Song, M., Wang, H. 2016.
1641 Oxidative stress and immunotoxicity induced by graphene oxide in zebrafish. *Aquat.*
1642 *Toxicol.*, 174, 54–60.
- 1643 Da Rocha, A.M., Ferreira, J.R., Barros, D.M., Pereira, T.C.B., Bogo, M.R.,
1644 Oliveira, S., Geraldo, V., Lacerda, R.G., Ferlauto, S., Ladeira, L.O., Veloso, M.,
1645 Pinheiro, V.B., Monserrat, J.M., 2013. Gene expression and biochemical responses in
1646 brain of zebrafish *Danio rerio* exposed to organic nanomaterials: Carbon nanotubes
1647 (SWCNT) and fullerenol (C60 (OH)18–22(OK4)). *Comp. Biochem. Physiol. A.*, 165,
1648 460–46.
- 1649 Dziewiecka, M., Karpeta-Kaczmarek, J., Augustyniak, M., Majchrzycki, L.,
1650 Augustyniak-Jabłokow, M.A., 2016. Evaluation of in vivo graphene oxide toxicity for
1651 *Acheta domesticus* in relation to nanomaterial purity and time passed from the exposure.
1652 *J. Hazard Mater.*, 305, 30–40.

- 1653 Esch C.d, Sliker, R., Wolterbeek, A., Woutersen, R., Groot, D.d. 2012. Zebrafish
1654 as potential model for developmental neurotoxicity testing: a mini review. *Neurotoxicol.*
1655 *Teratol.*, 34, 6, 545-553.
- 1656 Fako, V.E., Furgeson, D.Y., 2009. Zebrafish as a correlative and predictive model
1657 for assessing biomaterial nanotoxicity. *Adv. Drug Deliv. Rev.*, 61, 478–486.
- 1658 Firme, C.P. 3RD, Bandaru, P.R., 2010. Toxicity issues in the application of
1659 carbon nanotubes to biological systems. *Nanomed. Nanotechnol. Biol. Med.*, 6, 245–
1660 256.
- 1661 Fischer, H.C., Chan, W., 2007. Nanotoxicology: the growing need for in vivo
1662 study. *Curr. Opin. Biotechnol.*, 18, 565–571.
- 1663 Froehlicher M., Liedtke, A., Groh, K.J., Neuhauss, S.C., Segner, H., Eggen, R.I.,
1664 2009. Zebrafish (*Danio rerio*) neuromast: promising biological endpoint linking
1665 developmental and toxicological studies. *Aquat. Toxicol.*, 95, 307–19.
- 1666 He, J.H., Gao, J.M., Huang, C.J., Li, C.Q., 2014. Zebrafish models for assessing
1667 developmental and reproductive toxicity. *Neurotoxicol Teratol.*, 42, 35-42.
- 1668 Huang, C., Li, C., Shi G., 2012. Graphene based catalysts. *Energy Environ. Sci.*,
1669 5, 8848-8868.
- 1670 Iwai, M., 1973. Pesca exploratória e estudo biológico sobre camarão na costa
1671 centro-sul do Brasil do N/Oc.”Prof. W. Besnard” em 1969/71. São Paulo,
1672 SUDELPA/IOUSP. 71.
- 1673 Jortner, J., Rao, C.N.R., 2002. Nanostructured advanced materials. *Perspectives*
1674 *and directions. Pure Appl. Chem.*, 74, 1491–1506.

- 1675 Juarez-Moreno, K., Mejía-Ruiz, C.H., Díaz, F., Reyna-Verdugo, H., Re, A.D.,
1676 Vazquez-Felix, E.F., Sánchez-Castrejón, E., Mota-Morales, J.D., Pestryakov, A.,
1677 Bogdanchikova, N., 2017. Effect of silver nanoparticles on the metabolic rate,
1678 hematological response, and survival of juvenile white shrimp *Litopenaeus vannamei*.
1679 Chemosphere., 169, 716-724.
- 1680 Karlický, F., Datta, K.K.R., Otyepka, M., Zbořil, R., 2013. Halogenated
1681 graphenes: rapidly growing family of graphene derivatives, ACS Nano. 7, 6434–6464.
- 1682 Kiew, S.F., Kiew, L.V., Lee, H.B., Imae, T., Chung, L.Y., 2016. J. Control.
1683 Release, 226, 217–228.
- 1684 Kurantowicz, N., Strojny, B., Sawosz, E., Jaworski, S., Kutwin, M., Grodzik, M.,
1685 Wierzbicki, M., Lipińska, L., Mitura, K., Chwalibog, A., 2015. Biodistribution of a
1686 High Dose of Diamond, Graphite, and Graphene Oxide Nanoparticles After Multiple
1687 Intraperitoneal Injections in Rats. Nanoscale Res. Lett., 10(1), 398.
- 1688 Latin S., Henrard, L., 2006. Charge carriers in few-layer graphene films. Phys.
1689 Rev. Lett., 97, 0368031–0368034.
- 1690 Lawrence, C., 2007. The husbandry of zebrafish (*Danio rerio*): A review.
1691 Aquaculture, 269, 1–20.
- 1692 Lee, C.X., Wei, X.D., Kysar, J.W., Hone, J., 2008. Measurement of the elastic
1693 properties and intrinsic strength of monolayer graphene. Science, 321, 385-388.
- 1694 Liu, X., Sen, S., Liu, J., Kulaots, I., Geohegan, D., Kane, A., Poretzky, A.A.,
1695 Rouleau, C.M., More, K.L., Palmore, G.T., Hurt, R.H., 2011 (a). Antioxidant
1696 deactivation on graphenic nanocarbon surfaces. Small. 7, 19, 2775–2785.

- 1697 Liu, Z., Robinson, J.T., Tabakman, S.M., Yang, K., Dai, H., 2011 (b). Carbon
1698 materials for drug delivery & cancer therapy. *Mat. Today.*, 14, 316-323.
- 1699 Liu, S., Zeng, T.H., Hofmann, M., Burcombe, E., Wei, J., Jiang, R., Kong, J.,
1700 Chen, Y., 2011 (c). Antibacterial activity of graphite, graphite oxide, graphene oxide,
1701 and reduced graphene oxide: Membrane and oxidative stress. *ACS Nano.*, 5, 9, 6971–
1702 6980.
- 1703 Lobato, R.O., Nunes, S.M., Wasielesky, W., Fattorini, D., Regoli, F., Monserrat,
1704 J.M., Ventura-Lima, J., 2013. The role of lipoic acid in the protection against of metallic
1705 pollutant effects in the shrimp *Litopenaeus vannamei* (Crustacea, Decapoda). *Comp*
1706 *Biochem Physiol , A.*, 165(4), 491-497.
- 1707 Lotz, J.M., 1997. Effect of host size on virulence of Taura Virus to the marine
1708 shrimp *Penaeus vannamei* (Crustacea: Penaeidae). *Dis. Aquat. Org.*, 30, 45-51.
- 1709 Mao, L., Hu, M., Pan, B., Xie, Y., Petersen, E.J., 2016. Biodistribution and
1710 toxicity of radio-labeled few layer graphene in mice after intratracheal instillation. Part
1711 *Fibre Toxicol.*, 13, 7.
- 1712 Matés J.M, Pérez-Gómez C, Castro I.N., 1999. Antioxidant enzymes and human
1713 diseases. *Clin. Biochem.* 32, 595–603.
- 1714 Mieiro, M.P., Pereira, M.E., Duarte, A.C., 2011. Mercury organotropism in feral
1715 European sea bass (*Dicentrarchus labrax*). *Arch. Environ. Contam. Toxicol.*, 61, 1,
1716 135-43.
- 1717

- 1718 Monserrat, J.M., Martínez, P.E., Geracitano, L.A., Amado, L.L., Martins, C.M.G.,
1719 Pinho, G.L.L., Chaves, I.S., Ferreira-Cravo, M., Ventura-Lima, J., Bianchin, A., 2007.
1720 Pollution biomarkers in estuarine animals: Critical review and new perspectives. *Com.*
1721 *Biochem. Physiol., C.*, 146, 221-234.
- 1722 Nguyen, P., Berry, V., 2012. Graphene interfaced with biological cells:
1723 Opportunities and challenges. *The J. Phys. Chem. Lett.*, 3, 1024-1029.
- 1724 Oberdörster, E., 2004. Manufactured nanomaterials (fullerenes, C₆₀) induce
1725 oxidative stress in the brain of juvenile largemouth bass. *Envir. Hea. Perspec.*, 112,
1726 1058-1062.
- 1727 Pan, Y., Sahoo, N.G., Li, L., 2012. The application of graphene oxide in drug
1728 delivery. *Expert Opin Drug Deliv.*, 9, 1365-1376.
- 1729 Park, S., An, J., Jung, I., Piner, R.D., An, S.J., Li, X., Velamakanni, A., Ruoff,
1730 R.S., 2009. Colloidal suspensions of highly reduced graphene oxide in a wide variety of
1731 organic solvents. *Nano Lett.*, 9, 1593–1597.
- 1732 Park, S.; Mohanty, N., Suk, J.W., Nagaraja, A., An, J.H., Piner, R.D., Cai, W.W.,
1733 Dreyer, D.R., Berry, V., Ruoff, R.S., 2011. Biocompatible, robust free-standing paper
1734 composed of a TWEEN/graphene composite. *Adv. Mater.*, 22, 1736–1740.
- 1735 Perez-Farfante, I., 1969. Western Atlantic shrimp of the genus *Penaeus*. *Fish. Bull.*
1736 67, 3, 461-591.
- 1737 Pyati, U.J., Looka, A.T., Hammerschmidt, M., 2007. Zebrafish as a powerful
1738 vertebrate model system for in vivo studies of cell death. *Semin. Cancer Biol.*, 17, 154–
1739 165.

1740 Ren, X., Pan, L., Wang, L., 2015 (a). Toxic effects upon exposure to
1741 benzo[a]pyrene in juvenile white shrimp *Litopenaeus vannamei*. Environ. Toxicol.
1742 Pharmacol., 31, 194-207.

1743 Ren, X., Pan, L., Wang, L., 2015 (b). The detoxification process, bioaccumulation
1744 and damage effect in juvenile white shrimp *Litopenaeus vannamei* exposed to chrysene.
1745 Ecotoxicol. Environ. Safety, 114, 44-51.

1746 Silva, O., 1977. Aspectos bioecológicos e pesqueiros de três espécies de camarões
1747 do gênero *Penaeus* Costas do Estado do Rio de Janeiro e Experimentos de Cultivo, Rio
1748 de Janeiro, Universidade Federal do Rio de Janeiro.

1749 Storey, K.B. 2005. Functional Metabolism: Regulation and Adaptation. Ed. John
1750 Wiley & Sons. Hoboken, NJ.

1751 Strojny, B., Kurantowicz, N., Sawosz, E., Grodzik, M., Jaworski, S., Kutwin, M.,
1752 Wierzbicki, M., Hotowy, A., Lipińska, L., Chwalibog, A., 2015. PLoS One., 14. 10(12).

1753 Syama, S., Mohanan, P.V., 2016. Safety and biocompatibility of graphene: A new
1754 generation nanomaterial for biomedical application. Int. J. Biol. Macromolec., 86, 546–
1755 555.

1756 Texter, J., 2014. Graphene dispersions. Curr. Opin. Colloid Interface Sci. 19, 163–
1757 174.

1758 Usenko, C.Y., Harper, S.L., Tanguay R.L., 2008. Fullerene C60 exposure elicits
1759 an oxidative stress response in embryonic zebrafish. Toxicol. Appl. Pharmacol., 229, 44–
1760 55.

1761

- 1762 Ventura-Lima, J., Fattorini, D., Regoli, F., Monserrata, J.M., 2009. Effects of
1763 different inorganic arsenic species in *Cyprinus carpio* (Cyprinidae) tissues after short-
1764 time exposure: Bioaccumulation, biotransformation and biological responses. *Environ.*
1765 *Pollut.*, 157, 3479–3484.
- 1766 Zhang, X., Yin, J., Peng, C., Hu, W., Zhu, Z., Li, W., Fan, C., Huang, Q., 2011.
1767 Distribution and biocompatibility studies of graphene oxide in mice after intravenous
1768 administration. *Carbon*, 49, 986-995.
- 1769 Zhang, B. Wang, Y. Zhai, G., 2016. Biomedical applications of the graphene-
1770 based materials. *Mater. Sci. Eng., C.*, 61, 953–964.
- 1771 White, C.C, Viernes, H., Krejsa, C.M., Botta, D., Kavanagh, T.J. 2003.
1772 Fluorescence-based microtiter plate assay for glutamate-cysteine ligase activity. *Anal.*
1773 *Biochem.*, 318, 175-180.
- 1774 Yang, S.P., Wu, Z.H., Jian, J.C., Zhang, X.Z., 2010. Effect of marine red yeast
1775 *Rhodospiridium paludigenum* on growth and antioxidant competence of *Litopenaeus*
1776 *vannamei*. *Aquaculture*, 309, 62–65.
- 1777 Yang, K., Gong, H. Shi, X., Wan, J., Zhang, Y., Liu, Z., 2013. In vivo
1778 biodistribution and toxicology of functionalized nano-graphene oxide in mice after oral
1779 and intraperitoneal administration. *Biomaterials*, 34, 2787-2795.